AD-A092 738 PRINCETON UNIV NJ GUGGENHEIM AEROSPACE PROPULSION LABS F/G 21/2
MULTIPLE IGNITION, NORMAL AND CATALYTIC COMBUSTION AND QUENCHIN--ETC(U)
MAY 80 C BURNS, F V BRACCO, H S HOMAN AFOSR-76-3052
UNCLASSIFIED AFOSR-TR-80-1251 NL

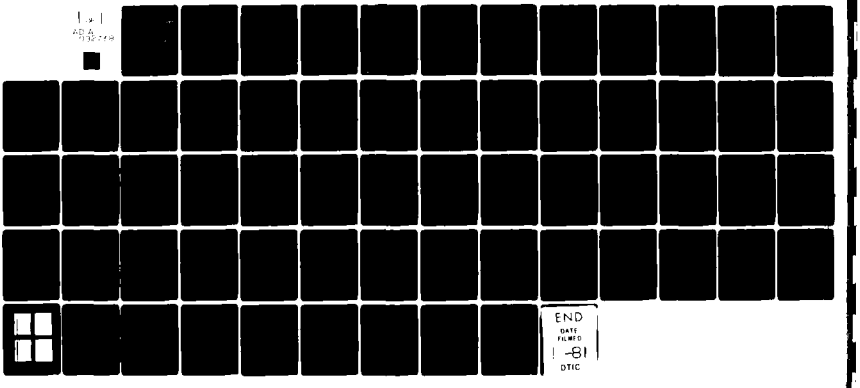

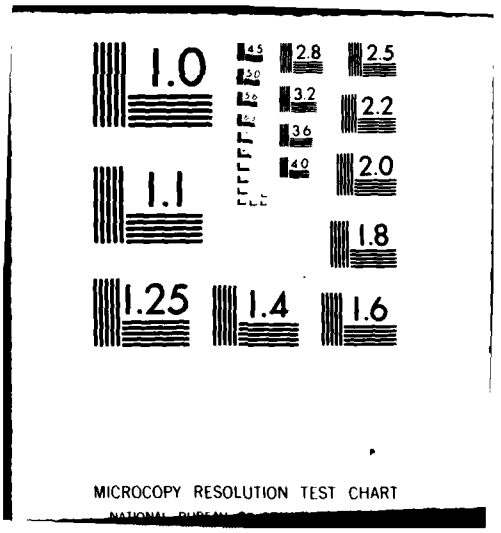
1.0
1.1
1.25
1.4
1.6
1.8
2.0
2.2
2.5
2.8
3.2
3.6
4.0
4.5
5.0
MICROCOPY RESOLUTION TEST CHART

AFOSR-TR- 80 - 1251

Annual Report
Air Force Systems Command
Air Force Office of Scientific Research

MULTIPLE IGNITION, NORMAL AND CATALYTIC COMBUSTION AND QUENCHING OF FUEL/AIR MIXTURES

F. V. Bracco and W. A. Sirignano
Principal Investigators

AFOSR-76-3052

Prepared by

C Burns
H. S. Homan
F. V. Bracco
W. A. Sirignano

10 May 1980

School of Engineering and Applied Science
Department of Mechanical and Aerospace Engineering
Guggenheim Aerospace Propulsion Laboratories
Princeton University
Princeton, New Jersey 08540

AIR FORCE OFFICE OF SCIENTIFIC RESEARCH (AFSC)
NOTICE OF TRANSMITTAL TO DDC
This technical report has been reviewed and is approved for public release IAW AFR 190-12 (7b).
Distribution is unlimited.
A. D. BLOSE
Technical Information Officer

SECURITY CLASSIFICATION OF THIS PAGE UNCLASSIFIED

REPORT DOCUMENTATION PAGE

READ INSTRUCTIONS BEFORE COMPLETING FORM

1. REPORT NUMBER (19) (18) AFOSR-TR-80-1251	2. GOVT ACCESSION NO. AD-A092738
3. RECIPIENT'S CATALOG NUMBER	
4. TITLE (and Subtitle) (6) Multiple Ignition, Normal and Catalytic Combustion and Quenching of Fuel/Air Mixtures.	5. TYPE OF REPORT & PERIOD COVERED Interim
	6. PERFORMING ORG. REPORT NUMBER
7. AUTHOR(s) (10) C. Bruno, H. S. Homan, F. V. Bracco, W. A. Sirignano	8. CONTRACT OR GRANT NUMBER(s) (15) AFOSR-76-3052
9. PERFORMING ORGANIZATION NAME AND ADDRESS Mechanical & Aerospace Engineering Dept. Princeton University Princeton, NJ 08544	10. PROGRAM ELEMENT, PROJECT, TASK AREA & WORK UNIT NUMBERS (16) 2308/A2 61102F
11. CONTROLLING OFFICE NAME AND ADDRESS Air Force Office of Scientific Research Bolling Air Force Base Washington, DC 20332	12. REPORT DATE (11) 10 May 1980
	13. NUMBER OF PAGES 50
14. MONITORING AGENCY NAME & ADDRESS (if different from Controlling Office) (12) 61 (17) A2	15. SECURITY CLASS. (of this report) UNCLASSIFIED
	15a. DECLASSIFICATION/DOWNGRADING SCHEDULE

16. DISTRIBUTION STATEMENT (of this Report)

Approved for public release; distribution unlimited

17. DISTRIBUTION STATEMENT (of the abstract entered in Block 20, if different from Report)

18. SUPPLEMENTARY NOTES

19. KEY WORDS (Continue on reverse side if necessary and identify by block number)

Catalytic Combustion
Metal Particles
Ignition

388 920

20. ABSTRACT (Continue on reverse side if necessary and identify by block number)

Lean combustion of propane in platinum/alumina/cordierite catalysts has been studied at atmospheric pressure, gas velocities of 10-40 m/s, C_3H_8 equivalence ratios of .19 to .32 and H_2O concentration of 1.2 to 1.7 mol %. Measurements of substrate temperature and gas composition, pressure, and temperature inside and downstream of the catalyst have been made. The dependences of substrate temperature, gas temperature, and gas composition on inlet temperature, reference velocity, and equivalence ratio have been investigated. A two-dimensional model of the gas-phase including the effect of finite-rate chemical

DD FORM 1 JAN 73 1473 EDITION OF 1 NOV 65 IS OBSOLETE

UNCLASSIFIED
SECURITY CLASSIFICATION OF THIS PAGE (When Data Entered)

20. Abstract (continued)

kinetics at the substrate surface has been developed and tested. When the experimental wall temperature is used as boundary condition for the gas-phase equations, the emission predictions are in reasonably good agreement with the measured ones. The indications obtained from the model are that propane is oxidized via a multi-step kinetic mechanism, that in the range of temperatures and equivalence ratios explored, most of the fuel is burnt at the catalytic wall rather than in the gas phase, and that wall kinetics is slower than gas diffusion transport.

Experimental data taken in Princeton facilities have been confirmed by data taken in CMU facilities using the same apparatus for ignition. These data indicate that a burning 40μ aluminum particle will ignite approximately stoichiometric mixtures of methane and air. Progressively larger particles are needed to ignite mixtures of increasing or decreasing fuel air equivalence ratio. Preparations to study ignition of toluene vapor and vapor/droplet systems have been made. A droplet generator has been acquired and tested. Appropriate modifications to the combustion chamber have been planned to allow study of small droplet systems. Characterization of sprays will involve use of standard techniques. Aluminum particle temperatures will be measured by multicolor pyrometry. Theoretical studies involving numerical integration of the governing equations and asymptotic analysis for high activation energy agree well with each other and with experiment. Minimum particle size as a function of particle temperature and as a function of mixture ratio are predicted.

STATEMENT OF WORK

AF FUNCTION - Weapon delivery and defenses, transport, advanced air-breathing engines, aircraft vulnerability and survivability.

DEFICIENCY - Insufficient understanding of the basic physical, chemical and fluid dynamic processes of (1) multiple ignition, propagation, and quenching of flames in spray-air mixtures and (2) of ignition, stability, and efficiency of catalytic combustion. Lack of guidelines for predicting potential flame/detonation quenching techniques and catalytic combustor performance and for solution of existing combustor difficulties.

OBJECTIVE - To clarify the relative importance, and to formulate realistic analytical representation of (1) the mechanisms of multiple ignition by hot metal particles, flame propagation and quenching in fuel-air sprays occurring in air-breathing propulsion system dry bays and fuel tanks, and (2) homogeneous, heterogeneous kinetics and transport processes in catalytic combustion phenomena associated with advanced air-breathing combustion systems.

HOW WORK CONTRIBUTES - Will provide additional understanding and needed realistic analytical modeling of multiple ignition, and flame propagation and attenuation through air-fuel sprays and of homogeneous and heterogeneous high temperature catalytic combustion processes not now available. Will contribute to establishing realistic guidelines and techniques for minimizing ignition probability and maximizing flame quenching and attenuation and for the design of efficient, stable, jet engine catalytic combustors.

APPROACH - Theoretical and experimental studies will be made of basic fluid dynamic, physical and chemical processes of ignition of hydrocarbon fuel sprays by clouds of hot metal particles acting as multiple ignition sources and associated combustion, detonation, and quenching in aircraft fuel tanks and dry bays, and of catalytic combustion associated with air-breathing propulsion systems. The relative importance of gas phase kinetics, heat transfer, mass diffusion, and surface chemical kinetics will be assessed. The practical phenomena will be experimentally simulated. The occurrence or absence of ignition of combustible gas by metal particles will be measured as a function of metal particle size, temperature, and gas-phase composition. Deficiencies in existing mathematical models will be demonstrated and improved models formulated based on experimental data and field observations. Concerning catalytic combustion, various monolithic and packed-bed catalyst candidates for advanced combustor design will be studied over a range of operating conditions characteristic of advanced air-breathing propulsion engines with various hydrocarbon fuels. A two-dimensional model for laminar and turbulent boundary layers with multiple gas and surface reactions will be formulated. Theoretical predictions will be made and compared with measurements of velocity, temperature, and concentrations within the boundary layer above the catalyst obtained by conventional and Raman, absorption and fluorescence laser techniques.

STATUS OF CATALYTIC COMBUSTION STUDY

During the period covered by this report, lean combustion of propane in a 24x24x76 mm platinum coated, alumina washcoated, cordierite substrate catalyst was studied.

A sketch of the experimental apparatus is shown in Figure 1. Preheated air at a measured flowrate is supplied to a 690 mm long test section with 25.4 mm square channel. A catalyst is pla ed with its downstream end 90 mm from the test section outlet, and insulated from the wall by Fiberfrax paper. Details of the catalyst section are shown in Figure 2. A fuel injector consisting of five 1.6 mm diameter tubes, each containing five 0.3 mm diameter holes, is located 440 mm from the catalyst inlet. A combination pitot tube and thermocouple is mounted 200 mm from the catalyst inlet. In addition to measuring gas velocity and temperature, the pitot tube is used to extract gas samples which are analyzed to determine equivalence ratio. Pressure is regulated by a valve in the exhaust pipe, and taps placed up and downstream of the catalyst are used to measure inlet pressure and pressure drop. A mass flowmeter (Hastings Model AHL-100P with H-3M/L-100 Transducer) measured the air flowrate. The water content of the inlet air was measured using a semiconductor sensor (Thunder Model 2000 with BR-101B probe) mounted in the airstream between the receiving tank and the heaters. The inlet conditions used in the experiments are summarized below.

Inlet temperature (T_{in}) = 650 ± 13 K to 800 ± 16 K
Inlet pressure (P_{in}) = 110 ± 5 kPa
Inlet Velocity (u_{in}) = 10 ± 4 to 40 ± 7 m/s
C_3H_8/air equivalence ratio (ϕ) = .19 ± .03 to .32 ± .04
H_2O = 1.2 ± .6 to 1.7 ± .6 mol%

A continuous effort was made to minimize crosswise gradients in temperature, velocity, and fuel concentration of the inlet stream. The entire test section is insulated so that uniform temperature across the width of the test section is obtained when sufficient time ($\sim$ 1 hr) has elapsed after startup of the air preheat system. Figure 3 shows velocity, temperature and propane concentration profiles obtained by traversing the width of the test section with the pitot/thermocouple probe. The uniformity is independent of air flowrate over the range of velocities used. Sufficient fuel/air mixing was obtained only by placing baffles downstream of the fuel injector, and these affect the velocity profile. By trying various configurations, the velocity uniformity was improved while maintaining an even distribution of fuel. The arrangement used in the present experiments consisted of two screens, each containing four 8 mm diameter

holes, placed 30 and 110 mm downstream of the fuel injector. Another screen perforated with 1.6 mm diameter holes was 190 mm from the injector and 50 mm upstream of the pitot tube. The resulting fuel distribution shows good uniformity over the measured range. Velocity profiles are less satisfactory (range ± 6% over 50% of the channel width). Average reference velocities were determined using the C_3H_8 and air flowrates, inlet temperature and pressure, and the cross section area of the catalyst. The catalyst inlet velocity, taking into account the fraction of open monolith area, is $u_{in} = (1.67 \pm .06)u_{ref}$.

Substrate temperatures were measured by a method similar to that described by Kesselring, Krill, and Kendall (1). Ni-Cr/Ni-Al thermocouples are fed through the test section wall and into the ends of catalyst channels. The lengths of wire inside the catalyst are covered by mullite insulator and both ends of the channel sealed with ceramic adhesive. The lifetime of these thermocouples under test conditions is short (5 - 20 hr). Exhaust gas samples were taken through an expansion quenched, water cooled, stainless steel probe mounted in an elbow downstream of the test section. Exhaust gas temperature was measured with a thermocouple mounted on the probe. CO and CO_2 were determined by infrared absorption (Horiba Model AIA-21), O_2 by magnetic susceptibility (Scott Model 250), and total hydrocarbon (HC, reported here as C_3) by a flame ionization detector (Scott Model 415). Pressure was measured inside the catalyst at 3 locations.

The catalyst was platinum supported on split cell corrugated Cordierite with γ-alumina washcoat. The overall dimensions of the monolith were 24 x 24 x 76 mm, the open area was 64%, the channel cross-section area was 1.9 mm^2, and the platinum loading was 4.2 kg/m^3. The physical properties of the catalyst are listed in Table 1. The sample was pretreated by burning propane for two hours with the maximum substrate temperature at 1480 K. The fuel was natural propane, 96 mole%, nominal.

The combustor was operated over a range of equivalence ratios, inlet temperatures and reference velocities at fixed inlet pressure. No attempt was made to minimize unburned fuel, since the objective was to understand the relationship between operating conditions and physico-chemical phenomena. Typical exhaust gas composition results are shown in Fig. 4, 5, 6 and 7. Fig. 4 shows CO formed by the C_3H_8 breakdown, being oxidized to CO_2 in the exhaust gas downstream of the catalyst.

A primary objective was the measurement of gas temperature and composition as functions of axial position inside a catalyst. This was accomplished by drilling an 8 mm diameter hole partway through the catalyst along its axis. The hole is lined with a ceramic sleeve to minimize the activity of the wall. A combination gas sampling and thermocouple probe is moved along the catalyst axis from downstream toward the bottom of the hole. If conditions are properly adjusted, the measured gas temperature and composition at the bottom of the hole are equal to their values at the same axial position in a catalyst with no hole. The condition which is most affected by the presence of the hole and probe is the gas velocity in the catalyst channels opening into the hole. The problem of establishing the correct velocity has been solved by feeding pressure taps through the side of the catalyst to measure the pressure at the bottom of the probe hole.

The velocity is adjusted until the pressure is equal to its value at the same axial position in a catalyst without a hole. Measured pressures show a linear decrease with increasing distance from the inlet during propane combustion in the Pt/Al_2O_3/Cordierite catalyst. Another requirement for reliable gas measurement inside a catalyst is that the substrate temperature be unaffected. This condition can also be satisfied despite the changed gas velocity because substrate temperature does not have a strong dependence on velocity. It is the constraint of fixed substrate temperature which distinguishes this experiment from one in which the overall length of catalyst is varied. In a catalyst of given length, the substrate temperature profile is different from the profile in an equivalent section of a longer catalyst. Direct measurements of fuel, oxygen, and product concentrations and gas temperature as functions of axial position inside a catalyst provide data for a rigorous test of a model for combustor operation. Calculations of species concentrations inside monolithic catalytic

combustors have been presented by Kelly, Kendall, Chu, and Kesselring (2) and by Cerkanowicz, Cole, and Stevens (3), but an experiment with which to compare these predictions had, to our knowledge, not yet been performed. Fig. 5 refers to results obtained from a catalyst with a hole depth equal to half the length of the catalyst. For the conditions of this experiment, fuel breaks down monotonically while at the same time the CO formed oxidizes to CO_2 and decreases as HC decreases.

Fig. 6 is interesting in the fact that while the UHC at the outlet keep decreasing with X, CO has a relative maximum. This is an indication that CO may be produced inside the catalyst at a rate larger than its rate of oxidation to CO_2.

This suspicion was confirmed by the results of Fig. 7, in which probing inside the hole revealed that not all the CO produced by propane pyrolysis is immediately oxidized to CO_2, and that a maximum exists inside the catalyst channels. More definite trends appear when temperatures and compositions are plotted versus inlet parameters. Fig. 8 has as parameter the inlet temperature. This has a strong effect on catalyst temperature and unburned HC at the outlet, which decreases rapidly as T_{in} is raised. However CO behaves non-monotonically: as T_{in} is raised, CO emissions at the outlet at first increase and then decrease.

The larger the UHC at the outlet, the higher the CO peak corresponding to HC breakdown to CO. From the figure it can be seen that the maxima of the rates of HC disappearance and CO production occur at approximately the same axial location.

The effect of varying equivalence ratio is shown in Fig. 9. Φ has a very strong influence on catalyst temperature, since it affects directly the adiabatic flame temperature, to which the wall temperature is close. For low Φ the UHC are relatively large at the outlet, and the low exhaust temperature results into low rates of HC breakdown into CO and CO oxidation. As Φ is increased both HC breakdown and CO oxidation proceed faster and faster: this seems to indicate that the CO axial peak tends to move inside the catalyst channels as Φ is raised.

Figs. 10a and 10b show the effect of varying inlet velocity and therefore residence time inside the channels. The wall temperature is only weakly affected by changing u_1, since it is always close to the adiabatic flame temperature corresponding to given T_{inlet} and Φ, which is independent of velocity. Emissions, instead, are strongly affected, and both UHC and CO become progressively larger as u_1 is increased. A maximum of CO at the outlet can be seen when u_1 is sufficiently high. This brief discussion of the experimental results points out the complexity of the interaction between physics and chemistry inside of the catalyst channels. The physical size of the probe used precluded a direct investigation inside an individual catalyst channel. What the probe could measure are quantities averaged over several channels cross sections, and no indication of radial diffusion effects could be obtained. A detailed description of these and other effects was supplied, however, by the mathematical model.

A sketch of the fundamental phsyico-chemical and fluid dynamics processes in a catalyst channel is shown in Fig. 11. The purpose of the model is to predict the effect of these processes on the exhaust products and the substrate. After reaching good agreement between predictions and experimental data, the model was used to investigate the relationship between the different processes.

For simplicity the catalyst channels are approximated by cylindrical channels. Preliminary results indicated that radiative heat transfer may be important at the two ends of the channel and for about 6% of the channel length. Therefore radiation is neglected in the model. With this simplification the equations describing catalytic combustion and the coordinate system are shown in Fig. 12 and Table 2 a,b.

These equations describe a two-dimensional, axisymmetrical, compressible, fluid flow with arbitrary chemical reactions in the gas phase, and with heat transfer and conduction in the substrate modeled assuming constant temperature across the substrate thickness s.

The reaction rates used in this study are shown in Table 3. The 3-step mechanism for propane oxidation in the gas phase was essential for a good agreement with the experimental data. (No reasonable results could be obtained by simply assuming C_3H_8 to break down into CO and then oxidizing CO to CO_2). This mechanism was obtained by Hautman et al. (4)(7) at Princeton and some slight adjustments were made to the activation energies and preexponential factors of reactions 1. and 2. These adjustments did not change the corresponding rates at the average temperature of the gas inside the pipe.

To test the validity of the model and separate gas phase effects from substrate effects, the gas phase equations were solved by uncoupling them from the substrate energy equation. In this case the only extra variable unknown is T_w, which was taken from the experiments and imposed as boundary condition at the wall. This procedure has as advantage the implicit inclusion of radiative effects in the model (provided the gas is optically thin), since the experimental wall temperature does include the effects of radiation.

The basic structure of the computer program used to solve the set of equations, "CATEACH", was based on the TEACH hydrodynamic code designed by A. D. Gosman and coworkers at The Imperial College. Details of CATEACH can be found in (5) and (6).

Some of the theoretical results are shown in Figs. 13 through 16 [see (6) for a detailed discussion]. Fig. 13 shows the monotonical decrease in HC concentration along the axis and from the axis to the catalytic wall. The rate of HC breakdown and oxidation is a function of the radial mass transfer and of the CO oxidation rate. Increasing the inlet velocity, as in Fig. 14, results in a correspondent decrease in residence time and a slower HC disappearance. Consistently, CO is still being formed at the outlet for this higher velocity case (see Fig. 15), and would presumable peak in the exhaust as in Fig. 10a. For the lower velocity case of Fig. 16, the residence time is sufficiently large for CO to begin to be oxidized inside the channel. Thus a relative CO maximum must occur, as in Fig. 5.

Overall comparison between theory and experiments is shown in Figs. 17 through 20. The pressure drop between catalyst inlet and outlet is important for gas turbine applications. There is a certain amount of disagreement between predictions and data; this is likely to be the effect of having approximated the [roughly] trapezoidal shape of the channel cross section by a circular one. The trends, however, are reproduced (see Fig. 17). Fig. 18 shows good agreement in the UHC comparison. Less satisfactory (but consistent as far as the trends) is the comparison for CO and CO_2 (see Figs. 19 and 20). It should be noted that the outlet emissions predictions are averages over the cross section, while data were taken with a probe hole slightly smaller than the channel size; part of the disagreement may be also due to radial gradients effects on the probe. A second cause may be a gradual loss of catalyst activity observed with increasing total run time (aging).

Once the computer code proved itself in predicting reasonable trends over the range of experimental measurement, some conclusions could be drawn. Fig. 21 shows the relative magnitude of gas phase vs. catalytic reaction rates. Most of the HC is oxidized at the catalytic wall, but this tends to change as the inlet temperature or the equivalence ratio is increased. The effect of velocity is opposite to the effect of inlet temperature but not as strong.

Figs. 22 a,b,c show the ratio between the characteristic wall kinetics time and the gas diffusion time for various velocities, inlet temperatures and equivalence ratios. In the ranges explored, the catalytic oxidation of C_3H_8 is slower than the C_3H_8 transport from the gas to the wall. However, the ratio is not everywhere in the channel large enough that radial diffusion may be considered infinitely fast (and the profiles assumed uniform in the radial direction).

In conclusion, the agreement between mathematical model and experimental data for C_3H_8 combustion in Pt/γ-Al_2O_3/cordierite monoliths is reasonably satisfactory. To recapitulate:

1. Substrate temperature is only weakly dependent on gas velocity.
2. Emissions depend strongly on all three parameters investigated.
3. Propane oxidation takes place via a multi-step mechanism involving at least three overall steps.
4. While unburned hydrocarbon varies monotonically with the three parameters investigated, CO emissions do not.
5. Most of the fuel is burned at the wall by catalyzed reactions rather than in the gas phase.
6. Radial gaseous diffusion is faster than heterogeneous kinetics.

STATUS OF MULTIPLE IGNITION STUDY

Burning aluminum particles have been used to ignite methane/air mixtures utilizing the apparatus shown in Figure 23. To briefly summarize its use a single aluminum particle of known size is suspended in the middle of the combustion chamber on the end of a glass fibre. The chamber is filled with the fuel-air mixture to be studied, and then is maneuvered by use of an x-y table so that the particle is placed in the path of a beam from a Nd:glass laser at the point where the beam is focused by the front lens. A pulse from the laser ignites the particle.

For a given run, three results are possible. First, the particle burns and ignites the mixture. Second, the particle burns but does not ignite the mixture. Third, neither the particle nor the mixture burns. It is possible to differentiate from among these possibilities using measurements which consist of a photograph of the chamber and a photographic record of oscilloscope traces from a photomultiplier tube and a pressure transducer. Burning gas is indicated by a large pressure signal increase, a large photomultiplier signal increase, and a totally exposed picture of the chamber. If the particle alone burns, this is indicated by a flat pressure signal, a photomultiplier trace with a small erratic jump shortly after the laser pulse, and a chamber photo with a small white spot. (The latter two effects both caused by burning of the particle.) A no-burn result is manifested by a flat pressure trace, a flat photomultiplier trace except for the initial laser pulse disturbance, and a tiny white spot on the chamber photo, coming from laser light reflected by the particle.

The most difficult determination is between a burning particle result and a no-burn result. For this determination, the photomultiplier trace is the essential piece of information. Figure 24 shows that a 40μ particle hit by the laser in an air atmosphere and one hit in a complete vacuum look very much

alike on the chamber photo. The photomultiplier trace for the particle hit in air, however, shows the previously discussed "blip" from burning that is absent from the trace for the particle shot in vacuum.

In determining minimum particle sizes to ignite a given mixture, it is imperative to use only sufficient energy to cause the particle to burn. Additional energy might heat the particle to a temperature higher than that achieved by ordinary combustion thus making gas ignition more likely. To ensure that only minimal laser energy is used, a series of runs is made for a given mixture and particle size. In each series, a high enough laser energy is used initially to cause the gas to ignite, whether due to burning of the particle alone or release of excess laser energy. In each successive run, the laser energy is reduced until a "no-burn" or a "particle-burn" result is obtained. A final run in which the particle burns but the gas does not ignite obviously means that the given particle (and those smaller than it) can burn in the given mixture without ignition because the heat release from the particle is not great enough. A final result of "no burn" (particle or gas) is slightly more subtle. This result implies that anytime the particle does burn, the gas ignites; a particle of the given size cannot burn in the given mixture without causing ignition. A summary of results obtained both at Princeton and CMU is shown in Figures 27 and 28 for methane-air and propane-air mixtures, respectively. These results will be briefly discussed in the following section.

The experiment will now begin focusing on fuel sprays. Toluene and tetralin have been selected as representative of high and low volatility aromatic liquids. The interest in aromatics is dictated by increasing interest in coal-derived liquids, which are often quite aromatic. The work will begin with an examination of toluene vapor-air studies similar to those on methane and propane. Under room temperature and pressure conditions, a saturated

air/toluene mixture has a fuel-air equivalence ratio of approximately 2.0. It will be possible to look at the critical diameter versus fuel-air equivalence ratio (ϕ) relationship from very lean mixtures up to this level of richness. These results will provide a baseline for comparison with later spray ignition results.

Spray systems will be produced using a TSI vibrating orifice aerosol generator. From a small liquid reservoir under high pressure, a liquid jet is forced thru a tiny orifice. The jet is made unstable by vibrations applied to the orifice plate, and the jet breaks up into a monodisperse spray. Variables to be investigated for spray systems include aluminum particle diameter, droplet size, number density, and overall fuel-air equivalence ratio. Overall ϕ is determined by the droplet number density for a given droplet size as the vapor phase ϕ is fixed by vapor-liquid equilibrium.

Two sets of combustion chamber modifications will be required to complete the study. For fine sprays (mists) in which the droplet settling velocities are slow and a spray will stay suspended for a reasonable length of time, a semi-batch test such as is used presently for vapors can be used. For larger droplets with high settling velocities, a flow-through procedure will be required. A procedure for handling fine sprays has been developed but has not yet been tested. As illustrated in Figure 25, the spray will be sent out of the generator into a mixing vessel equipped with tangential dispersion air jets. A line from the top of the mixing vessel to the combustion chamber will carry the spray. A line from the bottom of the chamber will lead to vacuum. To prepare a run, a particle will be suspended from the depth micrometer and properly positioned. While a steady state is being established, the system will operate continuously. The chamber inlet and outlet are closed. The laser is then fired.

The air supply for the tangential air jets on the mixing vessel and for the generator's dispersion air supply must be saturated with toluene to prevent evaporation of droplets. To provide this saturated air stream, a tower has been constructed to handle a sufficient flow rate. A gas chromatograph will be used to check the air stream for saturation.

It will be imperative to have a homogeneous mixture in the combustion chamber. To ensure that this is the case, an injection port has been installed on the droplet inlet line to the chamber. Smoke will be used to watch the flow characteristics in the chamber. Flow deflectors will be installed at the droplet inlet to correct inhomogeneities.

For a given test run, it will be necessary to know droplet size and droplet number density in the cumbustion chamber. Diameters of droplets greater than 10μ can easily be determined using a magnesium oxide test. A magnesium oxide coating is applied to a microscope slide. Droplets settling onto the slide leave an impression in the coating that can be measured under a microscope. Number densities can be measured using the apparatus shown in Figure 26. The attenuation of a (low power, continuous) laser beam passing through the spray is related to the concentration of droplets. The intensity of the laser beam passing through an empty chamber as measured with a photomultiplier tube and recorded on a digital ammeter is compared to that passing through a spray in the chamber to find beam attenuation.

Measurement of the aluminum particle surface temperature is considered to be an important addition to the experiment. The technique being tested involves use of a three-color pyrometer used at the U.S. Bureau of Mines for measuring the surface temperatures of dusts during explosions.

Analysis of Data

Figure 27 gives the methane/air data taken at Princeton and at CMU. The data compare favorably. Figure 28 gives the propane/air data taken at Princeton. No propane studies have been conducted at CMU. On each of these graphs, there are two curves. Curve I connects the largest particle sizes for which a "particle burn" result was obtained. Curve II connects the smallest particle sizes for which a "no burn" result was obtained. From the discussion in the previous section on experimental procedure, it should be clear that the actual ignition limit must lie somewhere between Curves I and II. Indeed, at a fuel equivalence ratio near one, 30μm particles sometimes gave "burn" and sometimes "no burn" results, implying that the true minimum size has been found at this equivalence ratio.

The number written above each data point gives the minimum laser voltage setting required to ignite a gas mixture with that ϕ value and that particle size. (Higher voltage setting gives superfluous energy: lower voltage setting yields a "no burn" or a "particle burn" result.) An interesting result is that for a given ϕ, the smallest of these minimum gas igniting laser voltage settings is found for the particle size on Curve I. For particles bigger than those on Curve I more energy than this minimum is required to ignite the particle. The combustion of these large particles then gives up more than enough energy to the gas to cause burning. A theoretical study by Su has shown that over the range of particle sizes studied in this experiment, the particle must burn to ignite the gas. Sufficient energy to ignite the gas is not available from even the largest particles studied if they are only heated but not burned. For particles smaller than those on Curve I, simply igniting the particle does not provide enough energy to burn the gas. Additional laser flux is required to heat the particle above the temperature at

which it would burn so that sufficient energy reaches the gas.

Under certain circumstances, an ignition delay between the burning of the particle and the burning of the gas in the chamber was observed. For propane/air mixtures, the trend was as follows. For particles greater than the critical size the gas combustion began immediately after the laser pulse as indicated by the photomultiplier tube trace. This result indicates that the gas ignites while the particle is still burning. For critically sized particles, however, tens of milliseconds passed between particle ignition and gas ignition. This result suggests that the particle must burn completely before the gas can ignite. This trend was observed for all values of ϕ studied. For methane/air mixtures a different trend was observed. For $\phi = 1.06$ and $\phi = 1.36$ data there was never an ignition delay even for the largest of particles.

Figure 29 and 30 show comparisons of the minimum size particle ignition data predicted by this experiment with the minimum spark ignition energies determined by Lewis and Von Elbe and with the minimum mass particle ignition data of Bowden and Lewis and of Liebman. Minimum particle mass (or size) can be easily converted to energy values using the product of mass (or volume times density) and heat of formation. These comparisons show that Lewis and Von Elbe's critical spark ignition energies are lower than the energies liberated by burning metal particles. For aluminum, the results show a close (within order of magnitude) agreement with spark ignition data. For other metals the agreement is not close. The relationship observed is that the minimum particle size required to ignite a given gas mixture is inversely proportional to the heat of formation of the metal. Bowden and Lewis obtained their data by placing metal particles on a hot nichrome ribbon in methane/air mixtures. They report no magnesium or aluminum data as they were unable to weigh particles of critical size. Liebman used laser ignition of electromagnetically

levitated particles.

An interesting contradiction presents itself in Figures 7 and 8. Because the burning of aluminum particles has been shown to be a diffusion-limited process, a region of oxygen depletion (locally high ϕ) is established near the burning particle. As a result, one would expect that the minimum in the critical size versus ϕ curve would be found for a leaner value of ϕ than the minimum in the spark ignition energy curve. For methane, however, the minimum in the two curves appears to coincide, and for propane the minimum in the particle size curve occurs at a higher value of ϕ than the minimum in the spark ignition energy curve.

The numerical and asymptotic studies of Su[8, 9, 10] support the general conclusions of the experimental research. A minimum particle size has been determined as a function of mixture ratio employing both one-step and four-step chemical kinetics for propane. See Figure 31. The agreement between theory and experiment is better with the particular four-step scheme which was employed although it is possible that an empirically-adjusted one-step non-second-order scheme might work just as well. Note that the smallest minimum particle size occurs on the fuel-rich side of stoichiometric for propane-air mixtures. It is also shown in Figure 32 that smaller particles require higher temperatures in order to ignite a given mixture.

In comparing asymptotic results with numerical results, it is found that in some cases, first order accuracy is insufficient and higher order analysis is required. The analysis has been carried to second order which usually is sufficient. Since many researchers are employing high-activation-energy asymptotics through first order only on a wide variety of combustion and ignition problems, these results have broad implications. Details are given in the references.

REFERENCES

1. Kesselring, J. P., W. V. Krill, and R. M. Kendall. Design Criteria for Stationary Source Catalytic Combustors. Presented at the Second EPA Workshop on Catalytic Combustion, Raleigh, NC, June 21-22, 1977.
2. Kelly, J. T., R. M. Kendall, E. Chu, and J. P. Kesselring. Development and Application of the PROF-HET Catalytic Combustor Code. Paper 77-33, Presented at the Fall 1977 Meeting, Western States Section, The Combustion Institute, Stanford, CA, October 17-18, 1977.
3. Cerkanowicz, A. E., R. B. Cole, and J. G. Stevens. Catalytic Combustion Modeling: Comparisons with Experimental Data. Presented at the ASME Gas Turbine Conference and Products Show, Philadelphia, PA, March 27-31, 1977.
4. Hautman, D. J., Hydrocarbon Oxidation Analysis. Paper presented at the Combustion Phenomena Contractors Review Meeting, U.S. Department of Energy, Pittsburgh Energy Technology Center, Pittsburgh, PA, Sept. 19, 1979.
5. Gosman, A. D., and F. J. K. Ideriah, "TEACH" - A General Computer Program for Two-Dimensional, Turbulent, Recirculating Flows. Dept. of Mech. Eng. Report, The Imperial College, London, SW7, 1976.
6. Yaw, Y., MSc Thesis, Princeton University, to be published.
7. Hautman, D. J., Pyrolysis and Oxidation Kinetic Mechanism for Propane, Ph.D. Thesis, Princeton University, 1980.
8. Su, Y. P., "Ignition of Combustible Mixtures by Metal Particles," Ph.D. Dissertation, Princeton University, August, 1980.
9. Su, Y. P., Homan, H. S., and Sirignano, W. A., "Numerical Predictions of Conditions for Ignition of a Combustible Gas by a Hot, Inert Particle," Combustion Science and Technology, Vol. 21, pp. 65-74, 1979.
10. Su, Y. P., and Sirignano, W. A., "Ignition of a Combustible Mixture by an Inert Hot Particle," to be published in Proceedings of the Eighteenth Combustion Symposium (1980).

PUBLICATIONS, PRESENTED PAPERS AND INTERACTIONS

"Breakthrough and Burnout of Carbon Monoxide in Catalytic Combustion," by P. M. Walsh, B. S. Kim, D. Santavicca and F. V. Bracco, presented at the 13th Middle Atlantic Meeting, American Chemical Society, March 19-23, 1979.

"Formation and Control of Fuel-Nitrogen Pollutants in Catalytic Combustion of Coal-Derived Gases," by B. S. Kim, Y. Yaw, D. Santavicca, P. M. Walsh, C. Bruno, and F. V. Bracco, presented at the U.S. DOE NO_x/SO_x Contractors' Meeting Morgantown Energy Technology Center, Morgantown, W. Va., Oct. 23-24, 1979.

"High Temperature Catalytic Combustion," by P. M. Walsh, C. Bruno, D. A. Santavicca, B. S. Kim and F. V. Bracco, presented at the 1980 AFOSR Contractors' Meeting on Air Breathing Combustion Dynamics and Kinetics, Alexandria, Va., Jan. 28-Feb. 1, 1980.

"Computed and Measured Emissions from the Catalytic Combustion of Propane/Air Mixtures," by F. V. Bracco, C. Bruno, Y. Yaw, and P. M. Walsh, presented at the 4th Workshop on Catalytic Combustion, U.S. EPA, Cincinnati, Ohio, May 14-15, 1980.

Dr. W. Pfefferle, one of the pioneers in catalytic combustion, is extremely interested in our program and has visited our laboratory a number of times for detailed discussion of our catalytic combustion program. Interest has also been shown by Professor T'ien, of Case-Western University, Dr. Osgerby of Engelhard Industries, Dr. Lavid, of Exxon Research and Engineering Company, and Dr. Bearden, of Dow Chemical. A presentation of this work was given at the IV EPA Workshop on Catalytic Combustion, May 1980.

"Numerical Predictions of Conditions for Ignition of a Combustible Gas by a Hot Inert Particle," by Y. P. Su, H. S. Homan, and W. A. Sirignano, Combustion Science and Technology, 1979, Vol 21, pp. 65-74.

"Minimum Mass of Burning Aluminum Particles for Ignition of Methane/Air and Propane/Air Mixtures," by Howard S. Homan and William A. Sirignano, to be published for The Eighteenth International Symposium on Combustion at Waterloo, Canada, August 17-22, 1980.

"Critical Initial Mass of Burning Aluminum Particles for Ignition of Methane/Air Mixtures," by Howard S. Homan, Samuel O. Morris, William A. Sirignano, preprinted for the 1979 Spring (Western States Section) Combustion Meeting, Provo, Utah, April 23, 24, 1979.

"Ignition of a Combustible Mixture by an Inert Hot Particle," by Yu-Pen Su and W. A. Sirignano, to be published in the Proceedings of the Eighteenth Combustion Symposium, 1980.

Interest in the ignition study has been demonstrated by Dr. Botteri and co-workers in the fuel systems group at Wright-Patterson. Mr. Mahood of Falcon Research and Development has also shown active interest. A number of requests for reprints and preprints have been received.

PERSONNEL

The following personnel have contributed to this research:

W. A. Sirignano, Professor, Co-Principal Investigator

F. V. Bracco, Associate Professor, Co-Principal Investigator

H. S. Homan, Research Staff Member

P. M. Walsh, Research Staff Member

C. Bruno, Research Staff Member

E. Suuberg, Assistant Professor

T. Stanley, Graduate Assistant

Table 1. Catalyst Properties

SUBSTRATE: Cordierite, American Lava Corp., AlSiMag 795, split cell

length 0.0760 ± 0.0003 m
wall thickness 0.25×10^{-3} m
open area 64%
channels per unit area 0.34×10^{6} m^{-2}
open area per channel 1.9×10^{-6} m^2
ratio surface area to total volume 2100 m^2/m^3
ratio surface area to gas volume 3260 m^2/m^3
channel hydraulic diameter (4/3260) 0.00123 m
bulk density 610 kg/m^3
solid density 1700 kg/m^3
safe operating temperature 1473 K
specific heat 800 J/kg•K
coefficient of thermal expansion (linear, 294 - 1033 K) 3.8×10^{-6} K^{-1}
thermal conductivity of solid (572 K) 1.4 J/m•s•K

approximate channel cross-section is a trapezoid with base lengths .0011 m and .0023 m, and height .0012 m

WASHCOAT: γ-alumina

loading 115-125 kg/m^3
surface area (BET) $(29.2 - 33.0) \times 10^{6}$ m^2/m^3

CATALYST: platinum

loading 4.2 kg/m^3
surface area (CO chemisorption) 6×10^{4} m^2/m^3

The γ-alumina and platinum were applied by Matthey Bishop, Inc., Malvern, PA.

Table 2a. Dimensional Governing Equations for Reacting Flow in a Circular Tube with Catalytic Wall.

$$\frac{\partial \rho}{\partial t} + \frac{1}{r}\frac{\partial \rho v r}{\partial r} + \frac{\partial \rho u}{\partial z} = 0 \qquad \text{continuity}$$

$$\frac{D\rho v}{Dt} = -\frac{\partial p}{\partial r} + \frac{1}{r}\frac{\partial \sigma_{rr} \cdot r}{\partial r} + \frac{\partial \sigma_{rz}}{\partial z} - \frac{\sigma_{\phi\phi}}{r} \qquad \text{radial momentum}$$

$$\frac{D\rho u}{Dt} = -\frac{\partial p}{\partial z} + \frac{1}{r}\frac{\partial \sigma_{rz}}{\partial r} + \frac{\partial \sigma_{zz}}{\partial z} \qquad \text{axial momentum}$$

$$\frac{D\rho h}{Dt} = \frac{\partial p}{\partial t} + \frac{1}{r}\frac{\partial}{\partial r}(\sigma_{rr} v r + \sigma_{rz} u r)$$

$$+ \frac{\partial}{\partial z}(\sigma_{rz} v + \sigma_{zz} u) - \frac{1}{r}\frac{\partial r q_r}{\partial r} - \frac{\partial q_z}{\partial z}$$

$$+ \sum_{\ell} Q_{\ell}\left[k_{f\ell} \prod_k \left(\frac{\rho_k}{W_k}\right)^{\nu'_{k\ell}} - k_{b\ell} \prod_k \left(\frac{\rho_k}{W_k}\right)^{\nu''_{k\ell}}\right] \qquad \text{energy}$$

$$\frac{D\rho k}{Dt} = \frac{1}{r}\frac{\partial}{\partial r}\left[\rho D_k r \frac{\partial (\rho_k/\rho)}{\partial r}\right] + \frac{\partial}{\partial z}\left[\rho D_k \frac{\partial (\rho_k/\rho)}{\partial z}\right] +$$

$$\sum_{\ell} W_k (\nu''_{k\ell} - \nu'_{k\ell})\left[k_{f\ell} \prod_k \left(\frac{\rho_k}{W_k}\right)^{\nu'_{k\ell}} - k_{b\ell} \prod_k \left(\frac{\rho_k}{W_k}\right)^{\nu''_{k\ell}}\right] \qquad \text{species}$$

$$p = \rho T R \Sigma (Y_k / W_k)$$

$$\frac{\partial T_w}{\partial t} = \frac{\partial^2 T_w}{\partial z^2} - \frac{2}{s}\frac{k}{k_w}\left[\frac{\partial T}{\partial r}\right]_{R^-} + \frac{2}{s k_w}\sum_{\ell} Q_{\ell} k_{f\ell} \prod_k \left(\frac{\rho_k}{W_k}\right)^{\nu_{k\ell}} \qquad \text{substrate energy}$$

Table 2b. Explanation of Symbols in Table 2a

C_p	specific heat at constant pressure (J/kg•K)
D	diffusion coefficient (m^2/s)
E	activation energy (J/mol)
h	enthalpy (J/Kg)
k	rate constant (cm^3/mol•s); Thermal conductivity (W/m•k)
Le	Lewis number = $\lambda/\rho DC_p$
P	pressure (Pa)
q	heat flux (J/m•s)
Q	heat of reaction (J/kg)
r	radial coordinate (m)
R	gas constant = 8.31 J/K•mol; pipe radius (m)
s	pipe thickness (m)
t	time (s)
T	temperature (K)
u	axial gas velocity (m/s)
v	radial gas velocity (m/s)
W	molecular weight
Y	mass fraction
z	axial coordinate (m)
ν', ν''	stoichiometric coefficients
ρ	density (kg/m^3)
σ	stress component (Pa)
ϕ	equivalence ratio
[ ]	concentration (mol/cm^3)

Subscripts

ad	adiabatic (reaction temperature)
b	backward reaction
f	forward reaction
in	condition at catalyst inlet
k	species k
ℓ	reaction ℓ
out	condition at catalyst outlet
r	radial
ref	reference condition (velocity)
w	wall
z	axial

Table 3

CHEMICAL REACTION RATE DATA USED IN THE MODELING OF 3-STEP KINETICS OF PROPANE OXIDATION ON $Pt/\gamma\text{-}Al_2O_3$/CORDIERITE CATALYST

REACTIONS

GAS	WALL
1. $C_3H_8 + \frac{1}{2} O_2 \rightarrow \frac{3}{2} C_2H_4 + H_2O$	1. $C_3H_8 + 5O_2 \rightarrow 3CO_2 + 4H_2O$
2. $C_2H_4 + 2O_2 \rightarrow 2CO + 2H_2O$	2. $C_2H_4 + 3O_2 \rightarrow 2CO_2 + 2H_2O$
3. $CO + \frac{1}{2} O_2 \rightarrow CO_2$	3. $CO + \frac{1}{2} O_2 \rightarrow CO_2$

RATES

GAS ($mol/cm^3 \cdot s$)	WALL ($mol/cm^2 Pt \cdot s$)
1. $1.4 \times 10^8 \exp(-40608/RT) \cdot ([C_3H_8]/[C_3H_8]_{in})^{.25} [O_2]^{1.04}$	1. $1.09 \times 10^9 \exp(-17600/RT)[C_3H_8]$
2. $4.8 \times 10^{14} \exp(-70000/RT) \cdot ([C_2H_4]/[C_3H_8]_{in})^{.96} [O_2]^{1.18}$	2. $10^{7.04} \exp(-12000/RT)[C_2H_4]$
3. $1.0 \times 10^{10} \exp(-30000/RT) \cdot [CO][O_2]^{.25} [H_2O]^{.5}$	3. $3.83 \times 10^3 \exp(-24900/RT)[CO]$

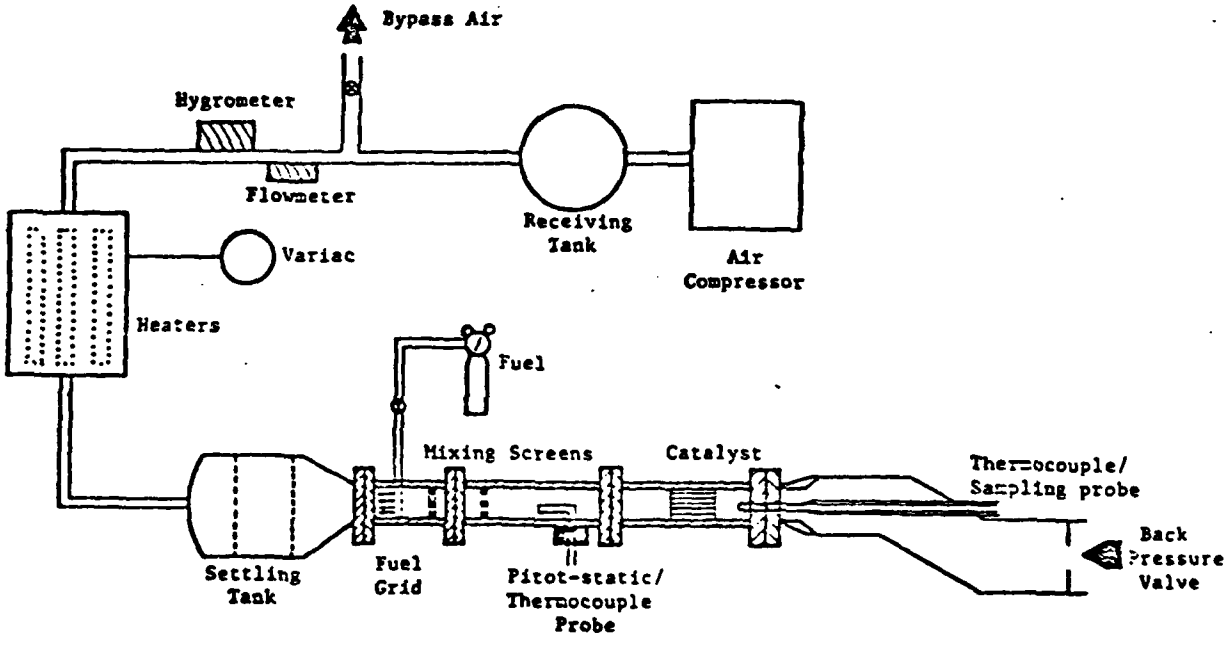

FIGURE 1. SCHEMATIC DIAGRAM OF THE FLOW REACTOR WITH CATALYTIC COMBUSTION TEST SECTION

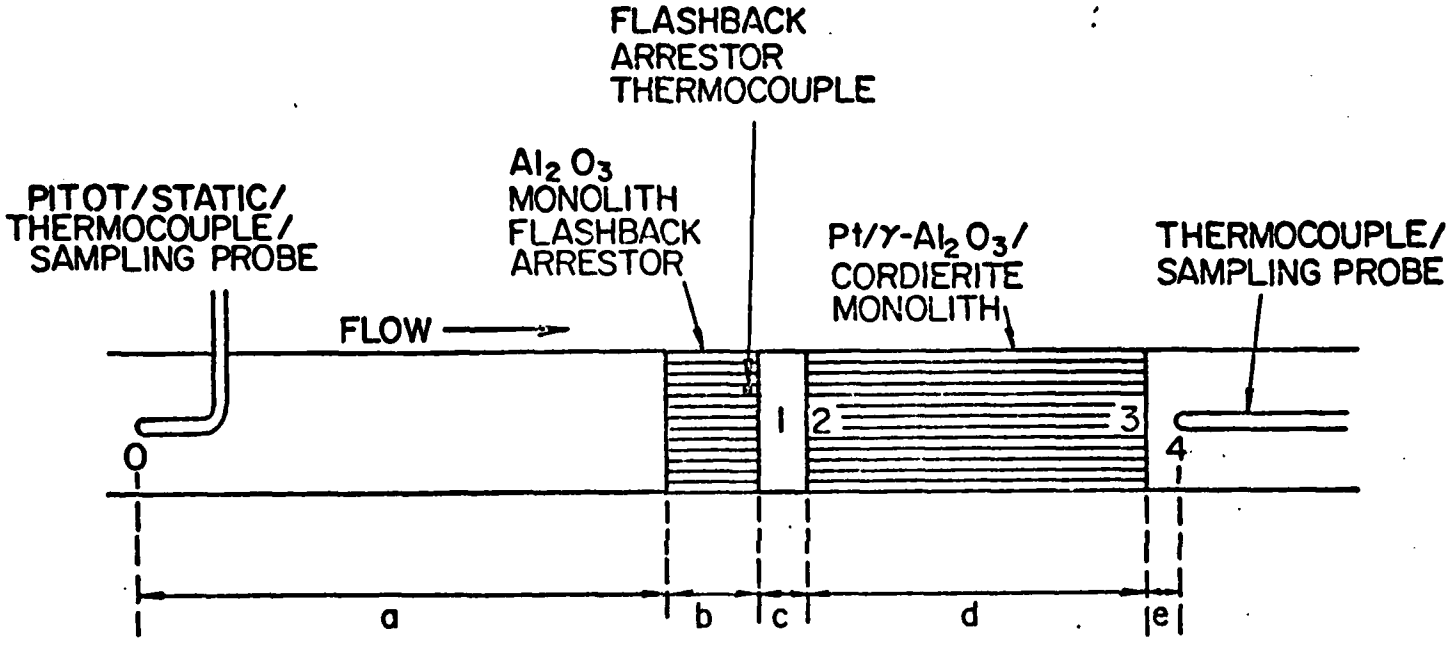

a 0.217 ± 0.001 m

b 0.0132 OR 0.0262 ± 0.0003 OR 0

c 0.001 TO 0.003

d 0.0760 ± 0.0003

e 0.0010 ± 0.0005

FIGURE 2. DETAILS OF THE CATALYST TEST SECTION.

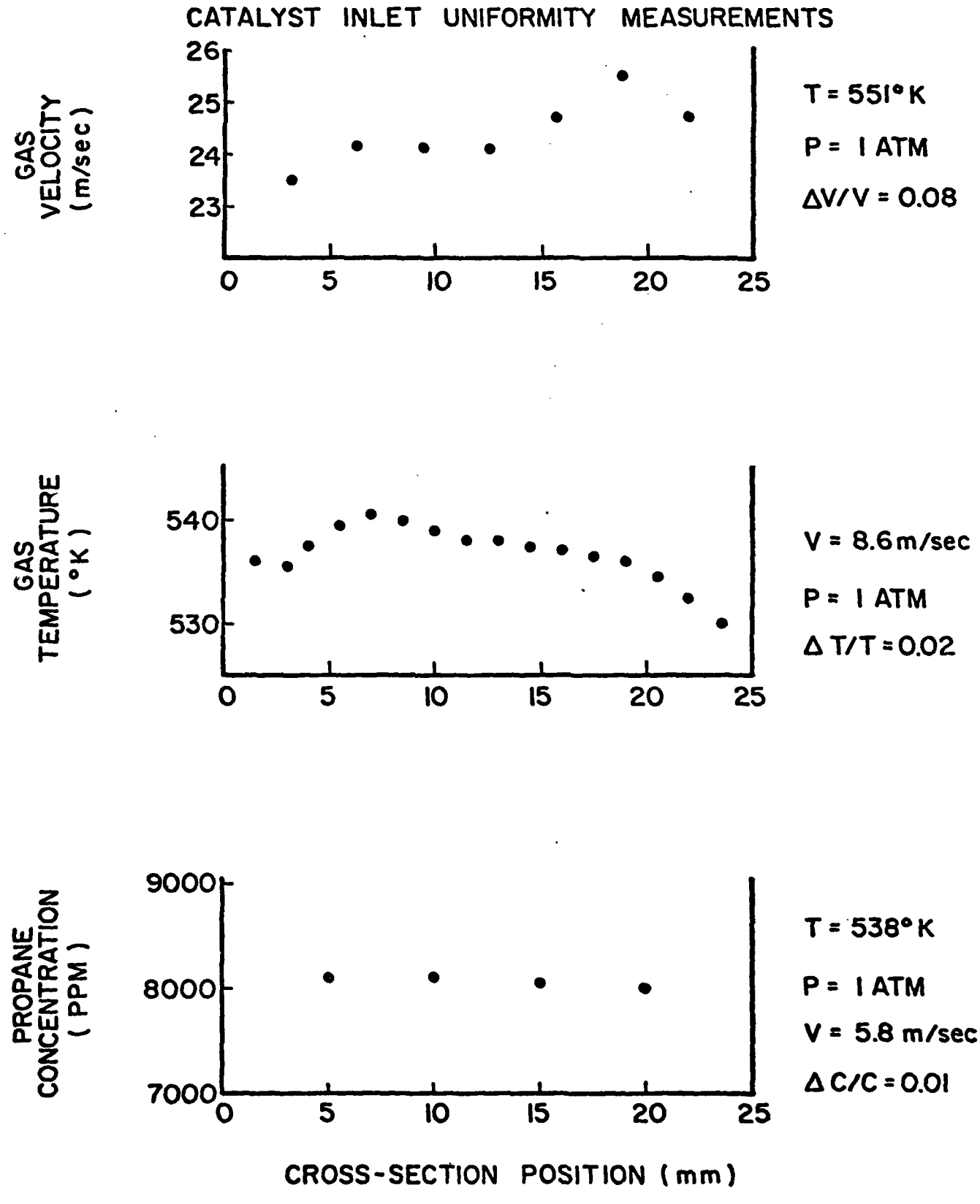

FIGURE 3. UNIFORMITY MEASUREMENTS ACROSS THE TEST SECTION LOCATION 0.

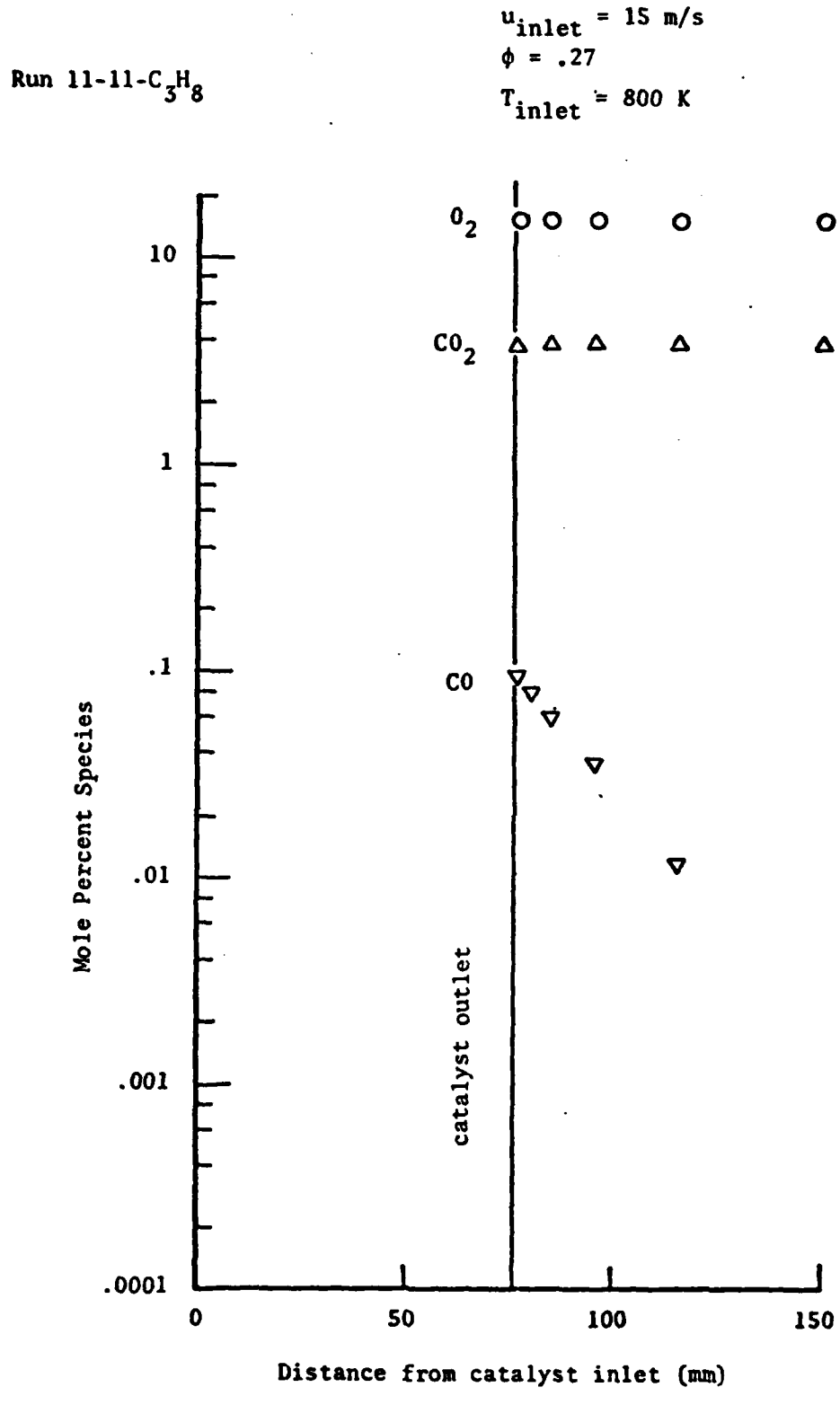

FIGURE 4. EXHAUST GAS COMPOSITION DOWNSTREAM OF THE CATALYST.

Run 11-13-C_3H_8

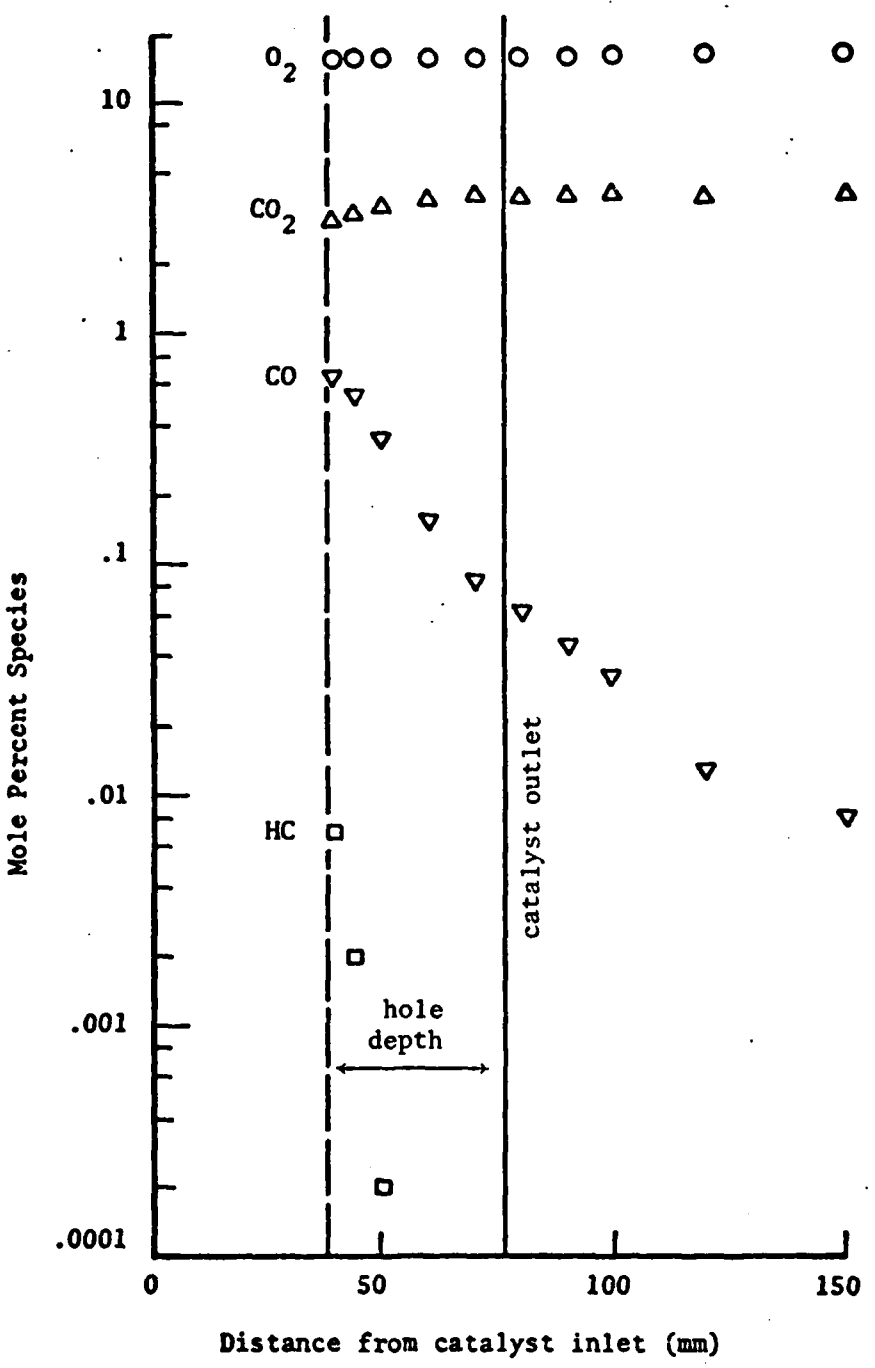

FIGURE 5. EXHAUST GAS COMPOSITION INSIDE AND DOWNSTREAM OF THE CATALYST.

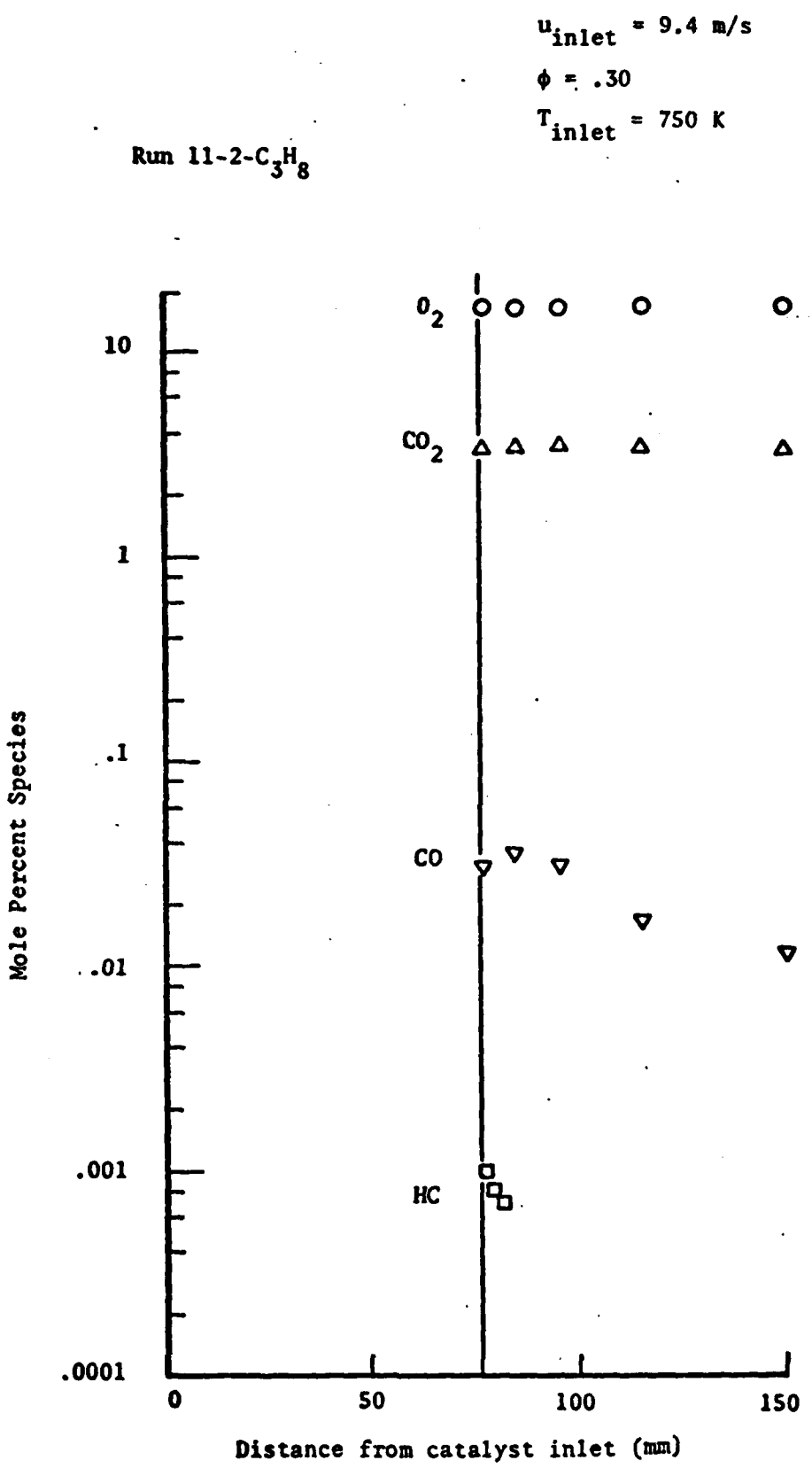

FIGURE 6. EXHAUST GAS COMPOSITION DOWNSTREAM OF THE CATALYST.

$u_{inlet} \approx 6.4$ m/s

$\phi = .28$

$T_{inlet} \approx 800$ K

Run 11-15-C_3H_8

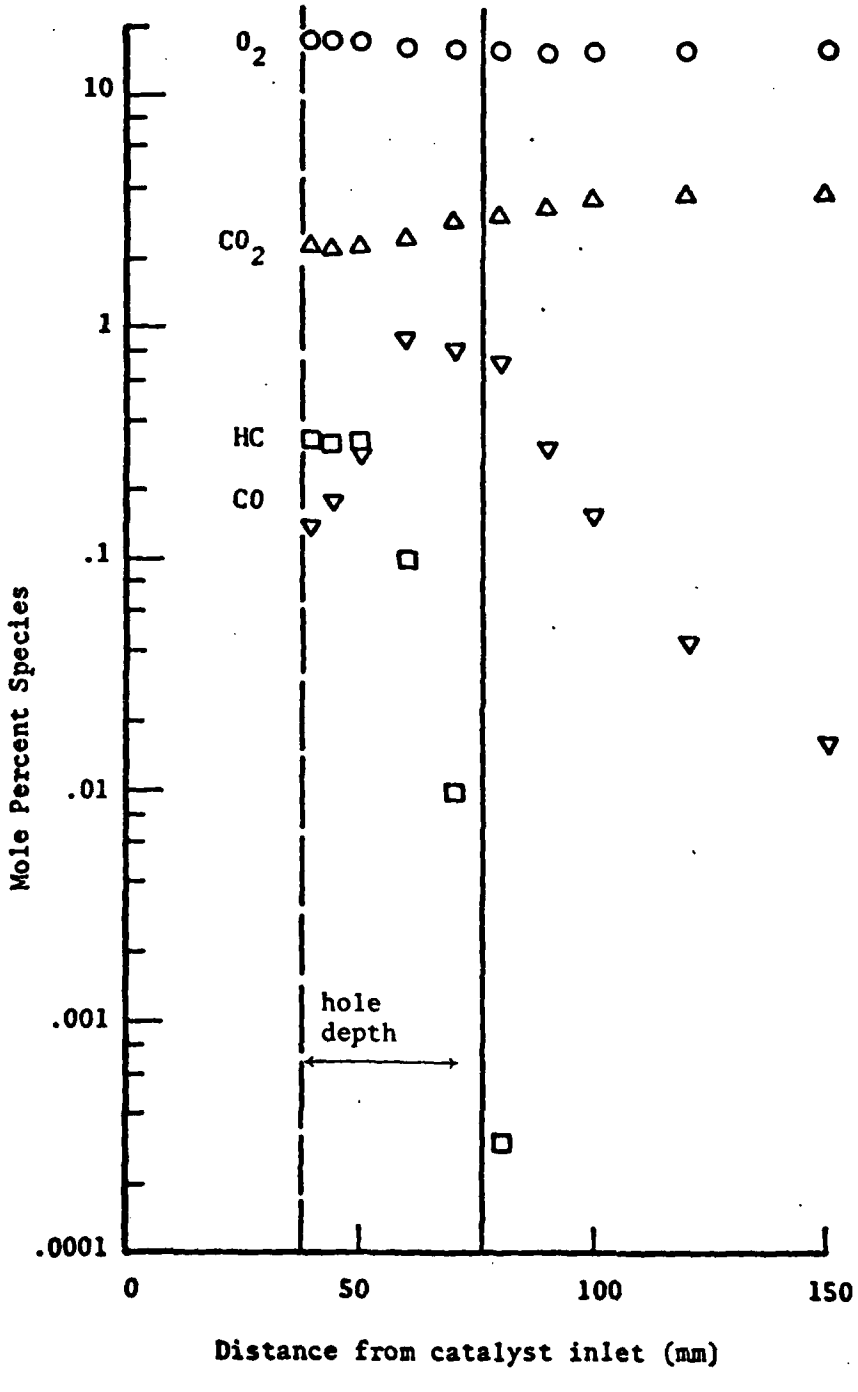

FIGURE 7. EXHAUST GAS COMPOSITION INSIDE AND DOWNSTREAM OF THE CATALYST.

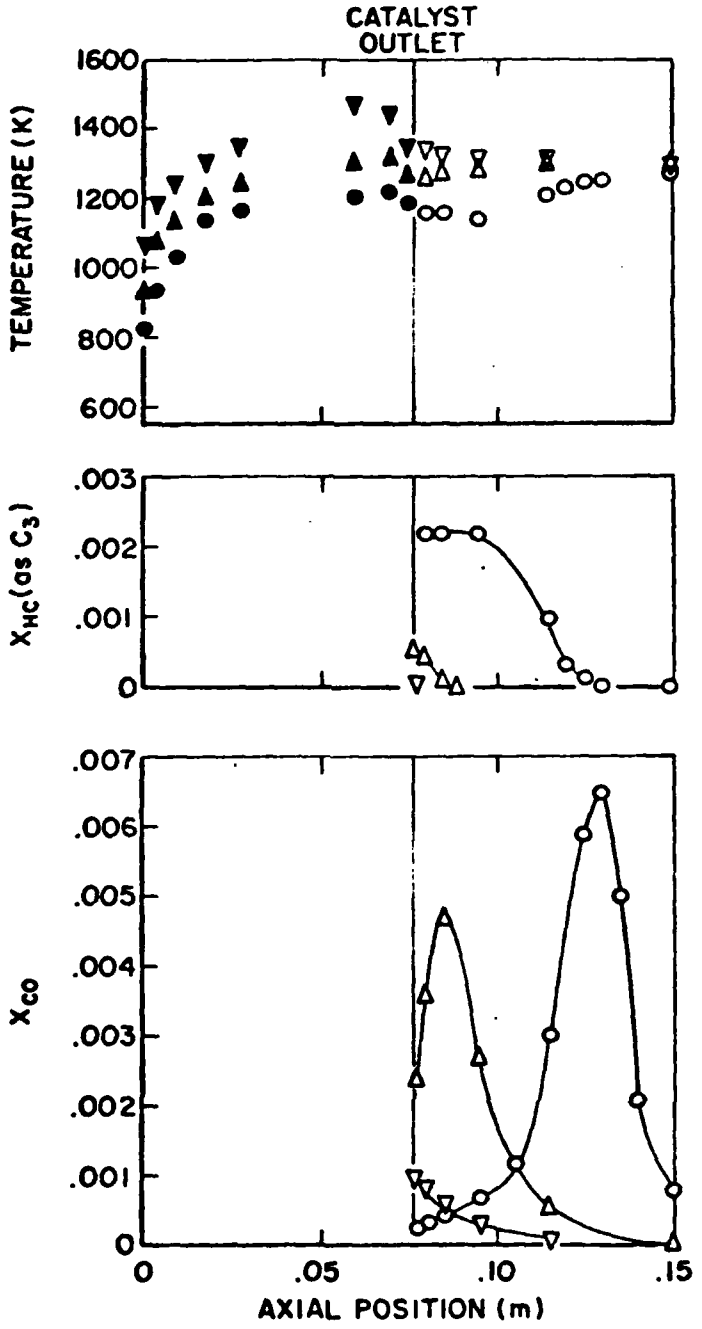

FIGURE 8. TEMPERATURE ANDCOMPOSITION AS A FUNCTION OF T_{INLET}.

SOLID	GAS	T_o(K)
●	○	650±13
▲	△	700±14
▼	▽	800±15

$P_o = 110 \pm 5$ kPa

$\phi = 0.28 \pm 0.05$ $\langle u_p \rangle = 15 \pm 5$ m/s

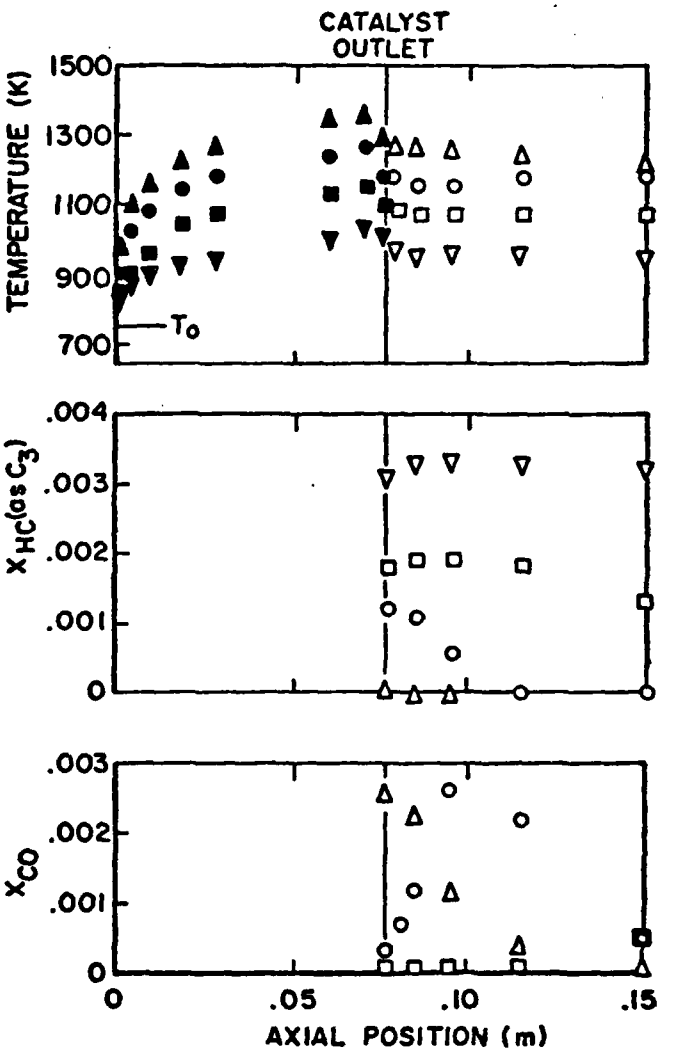

FIGURE 9. TEMPERATURE AND COMPOSITION AS A FUNCTION OF ϕ.

SOLID	GAS	ϕ
▼	▽	0.19 ± .03
■	□	0.22 ± .04
●	○	0.25 ± .05
▲	△	0.28 ± .05

$P_o = 110 \pm 5$ kPa

$T_o = 750 \pm 14$ K

$\langle u_i \rangle = 15 \pm 5$ m/s

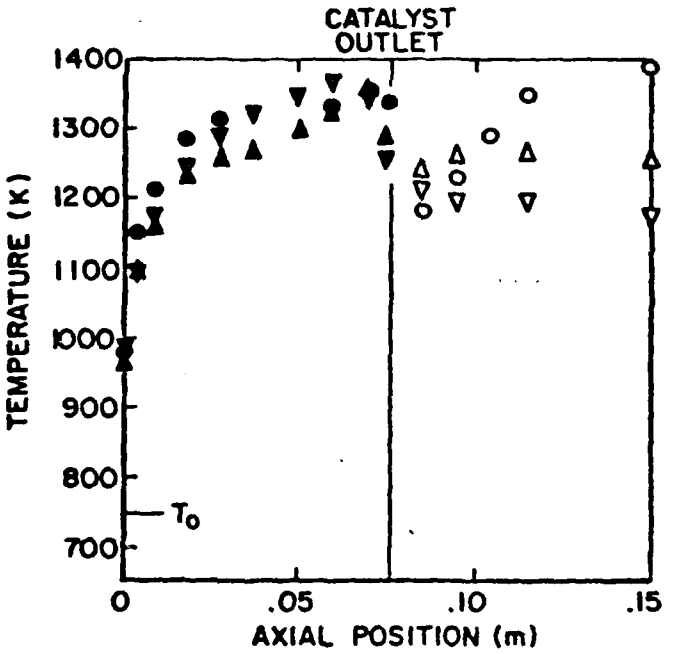

FIGURE 10a. TEMPERATURE AS A FUNCTION OF INLET VELOCITY u_1.

SOLID	GAS	$\langle u_1 \rangle$ (m/s)
▼	▽	10±4
▲	△	20±5
●	○	40±7

$P_0 = 110 \pm 5$ kPa
$T_0 = 750 \pm 14$ K
$\phi = 0.30 \pm 0.07$

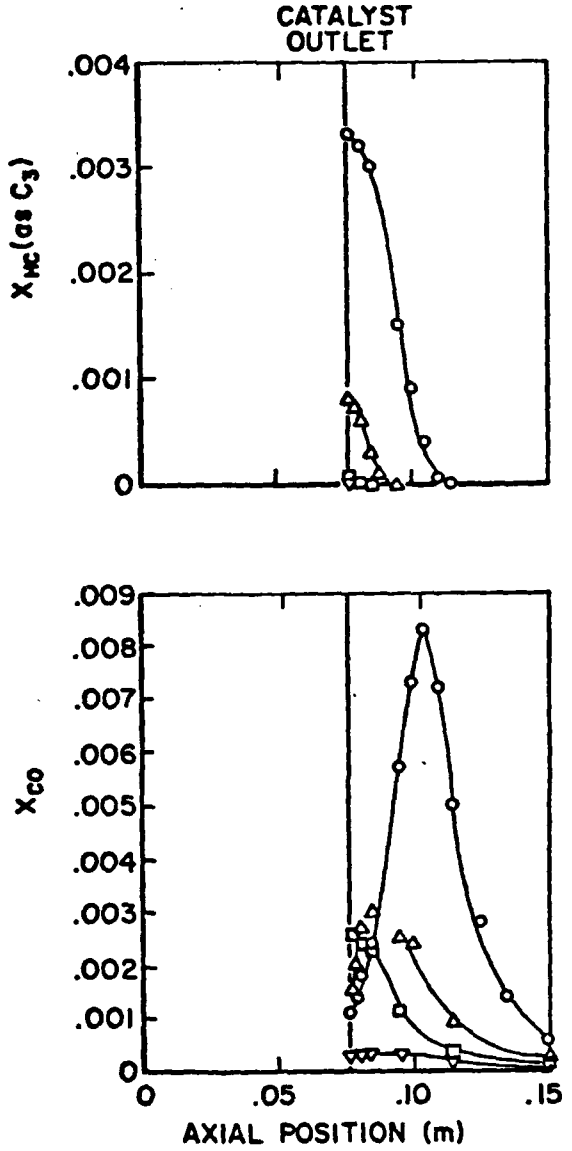

FIGURE 10b. COMPOSITION AS A FUNCTION OF INLET VELOCITY u_1.

	$\langle u_1 \rangle$ (m/s)
▽	10 ± 4
□	15 ± 5
△	20 ± 5
○	40 ± 7

$P_0 = 110 \pm 5$ kPa

$T_0 = 750 \pm 14$ K

$\phi = 0.30 \pm 0.07$

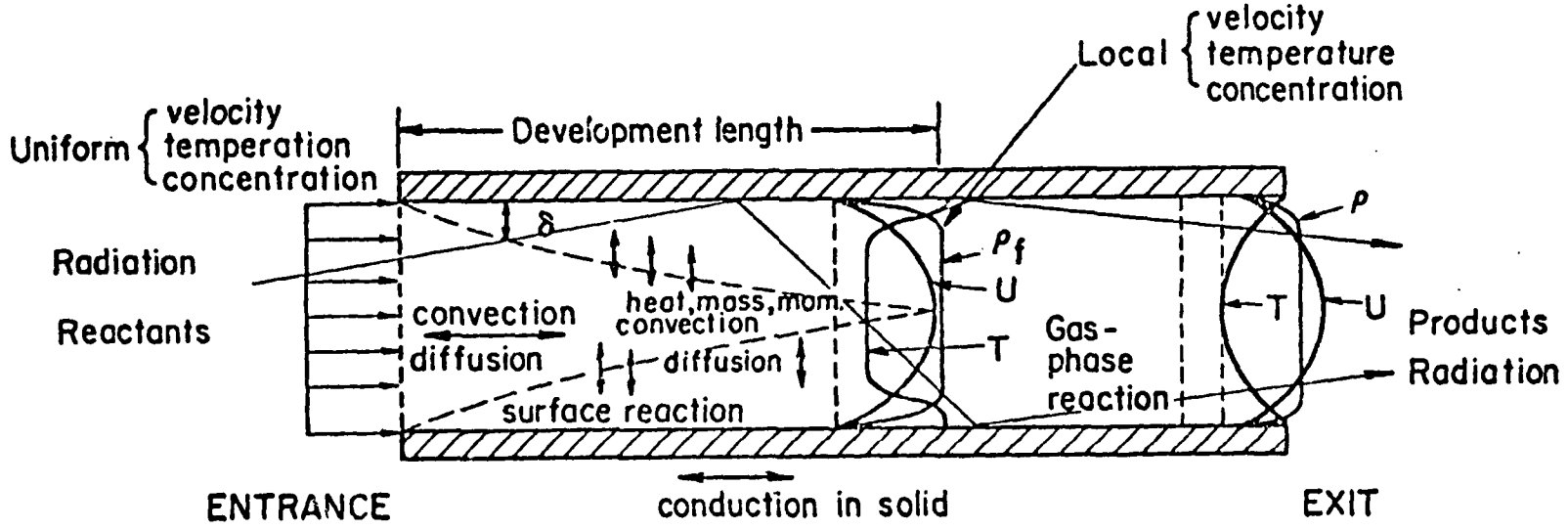

FIGURE 11. PHYSICAL AND CHEMICAL PROCESSES IN A CHANNEL OF CATALYST.

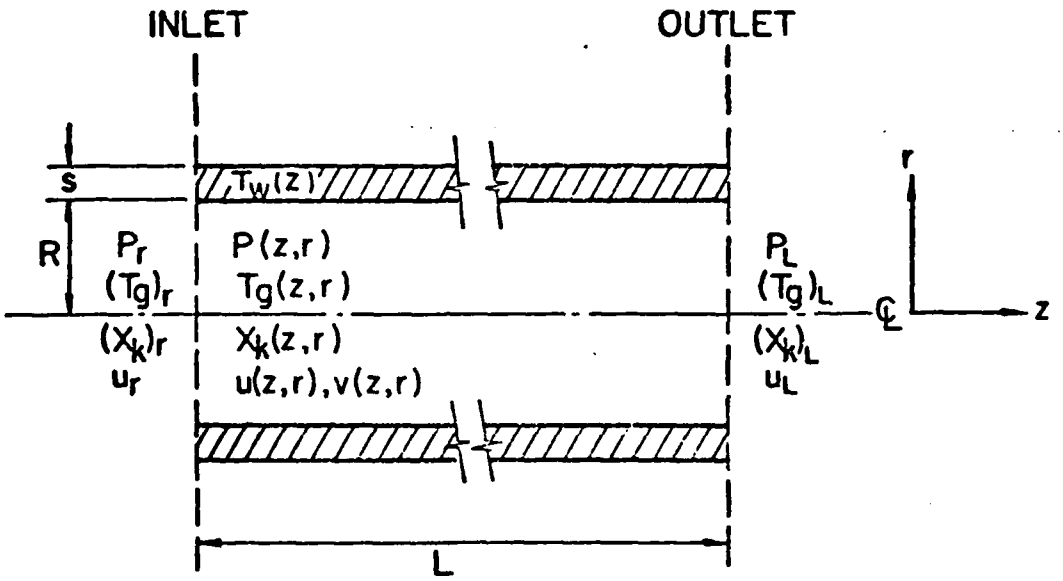

FIGURE 12. COORDINATE SYSTEM AND VARIABLES IN THE MODEL OF A CATALYST CHANNEL.

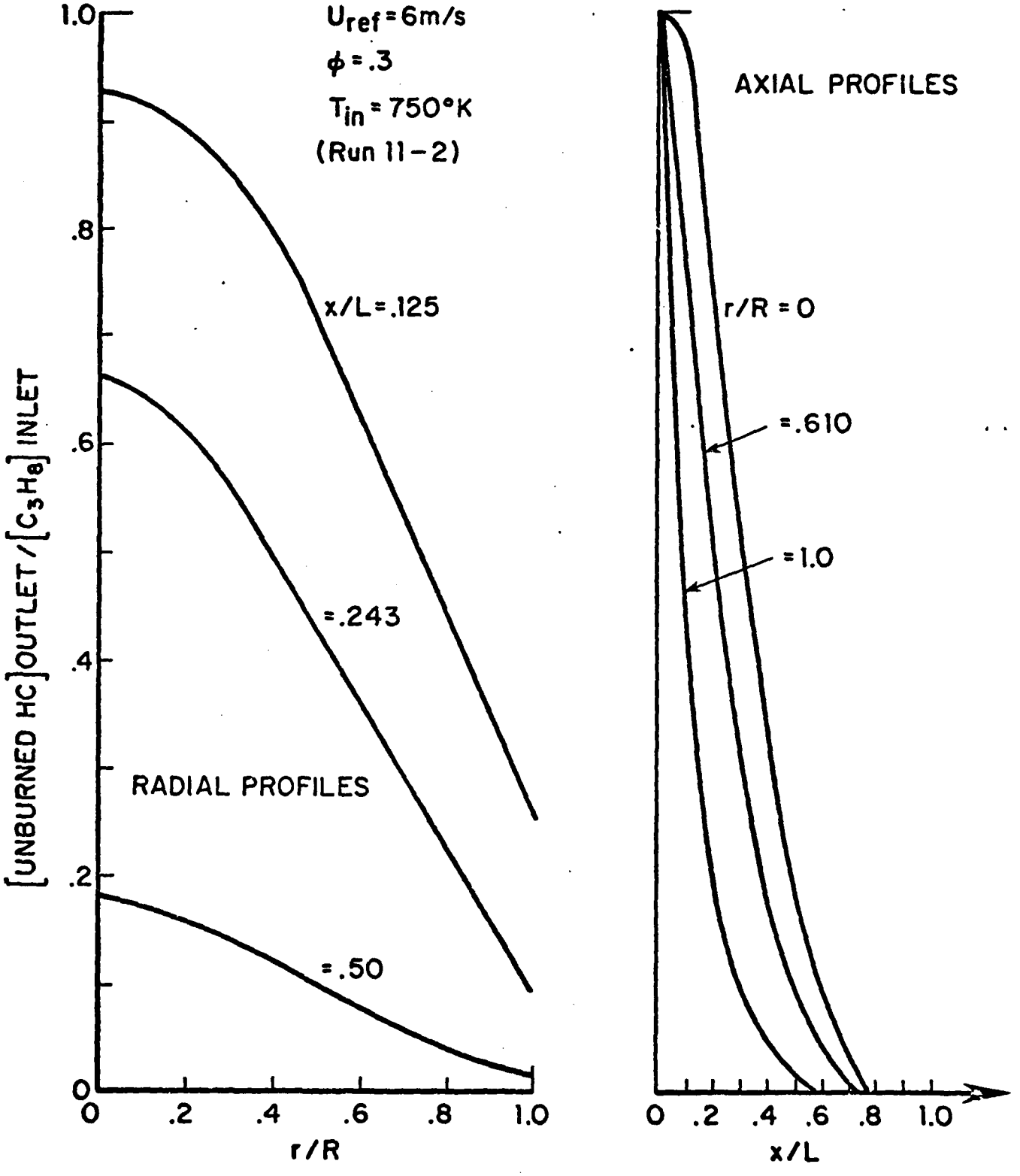

FIGURE 13. THEORETICAL PROFILES OF UNBURNED HC VS. r AND x FOR 3-STEP (OVERALL) CATALYTIC OXIDATION OF C_3H_8

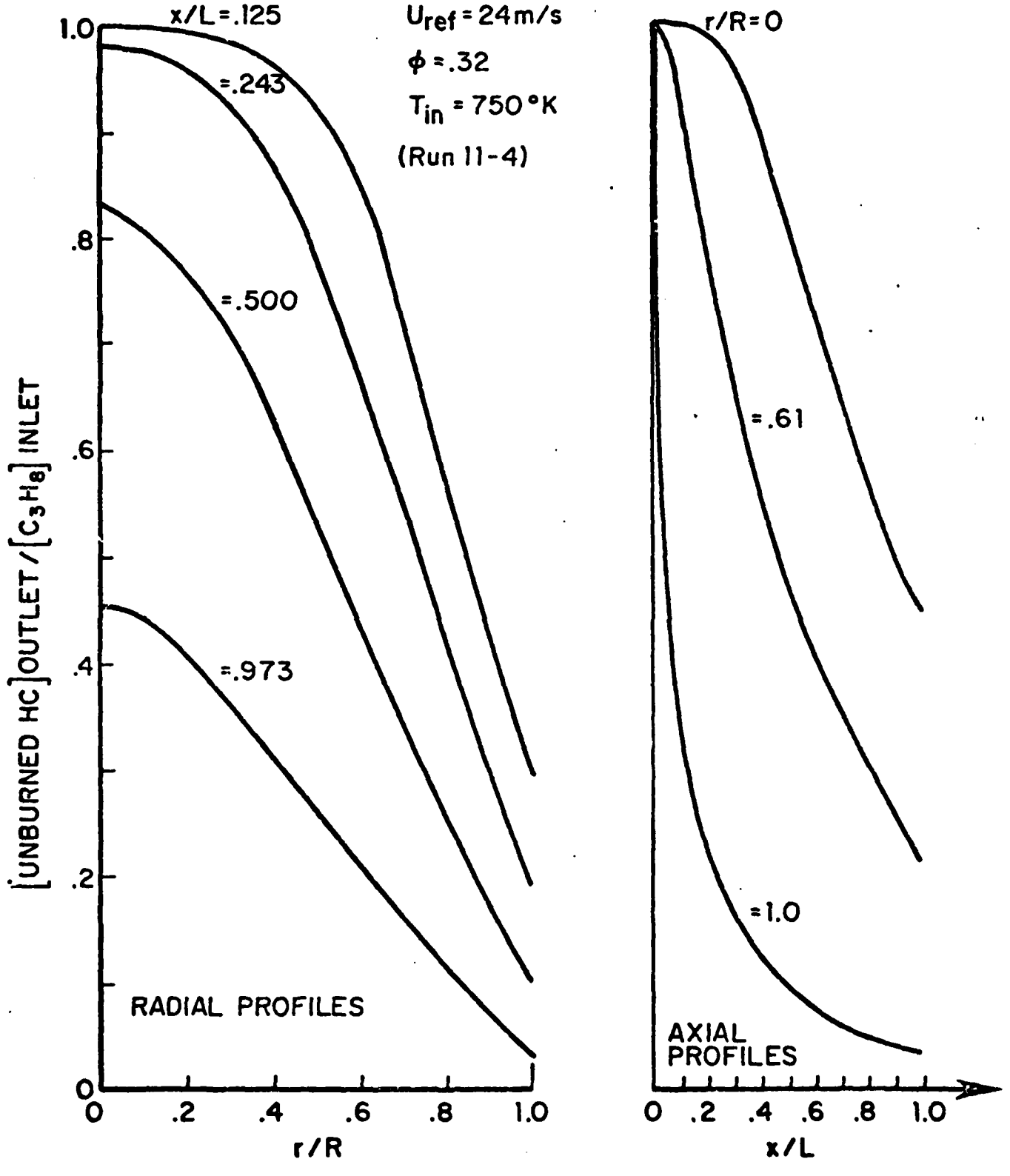

FIGURE 14. THEORETICAL PROFILES OF UNBURNED HC VS. r AND x FOR 3-STEP (OVERALL) CATALYTIC OXIDATION OF C_3H_8

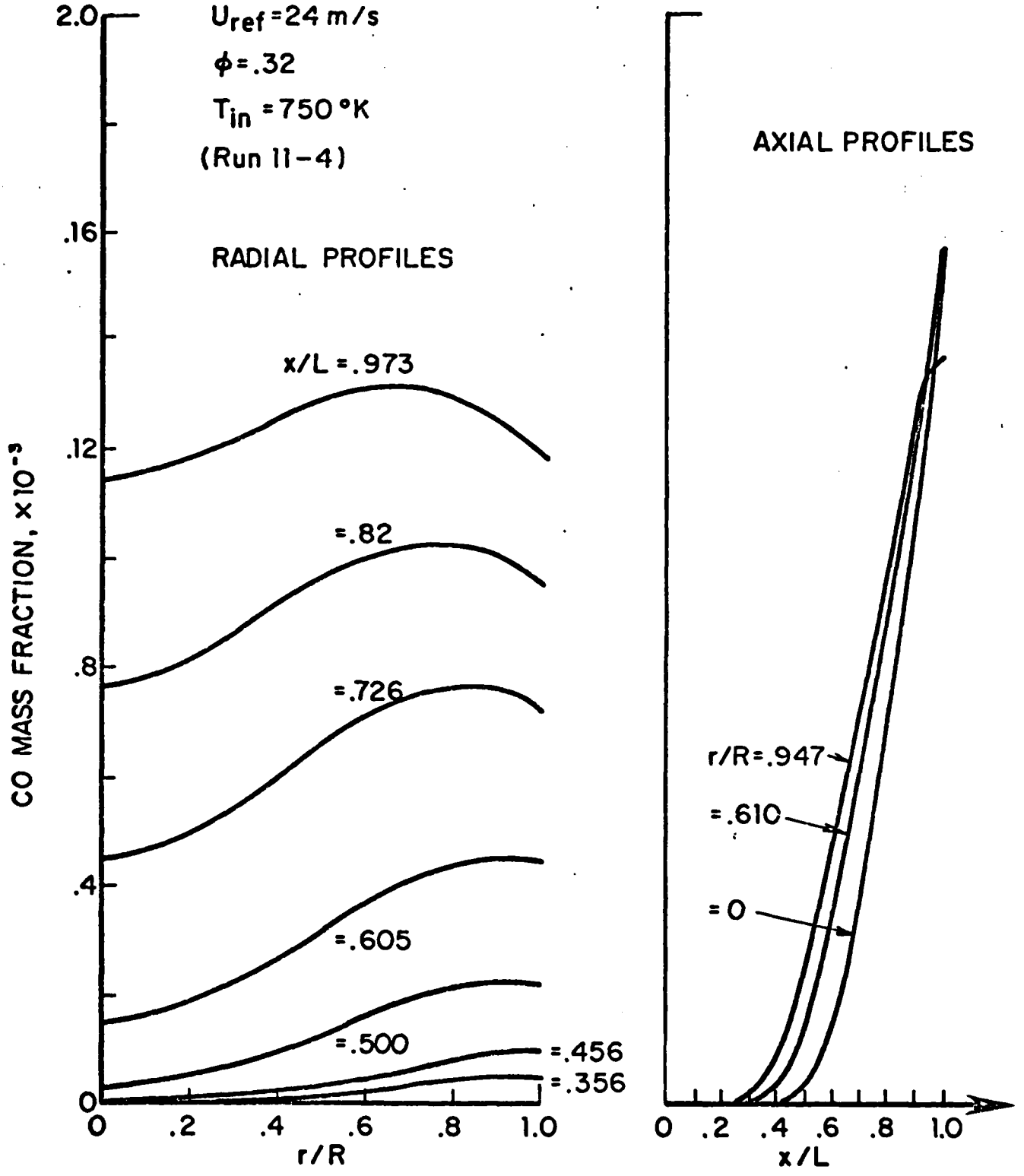

FIGURE 15. THEORETICAL PROFILES OF CO VS. r AND x FOR 3-STEP (OVERALL) CATALYTIC OXIDATION OF C_3H_8

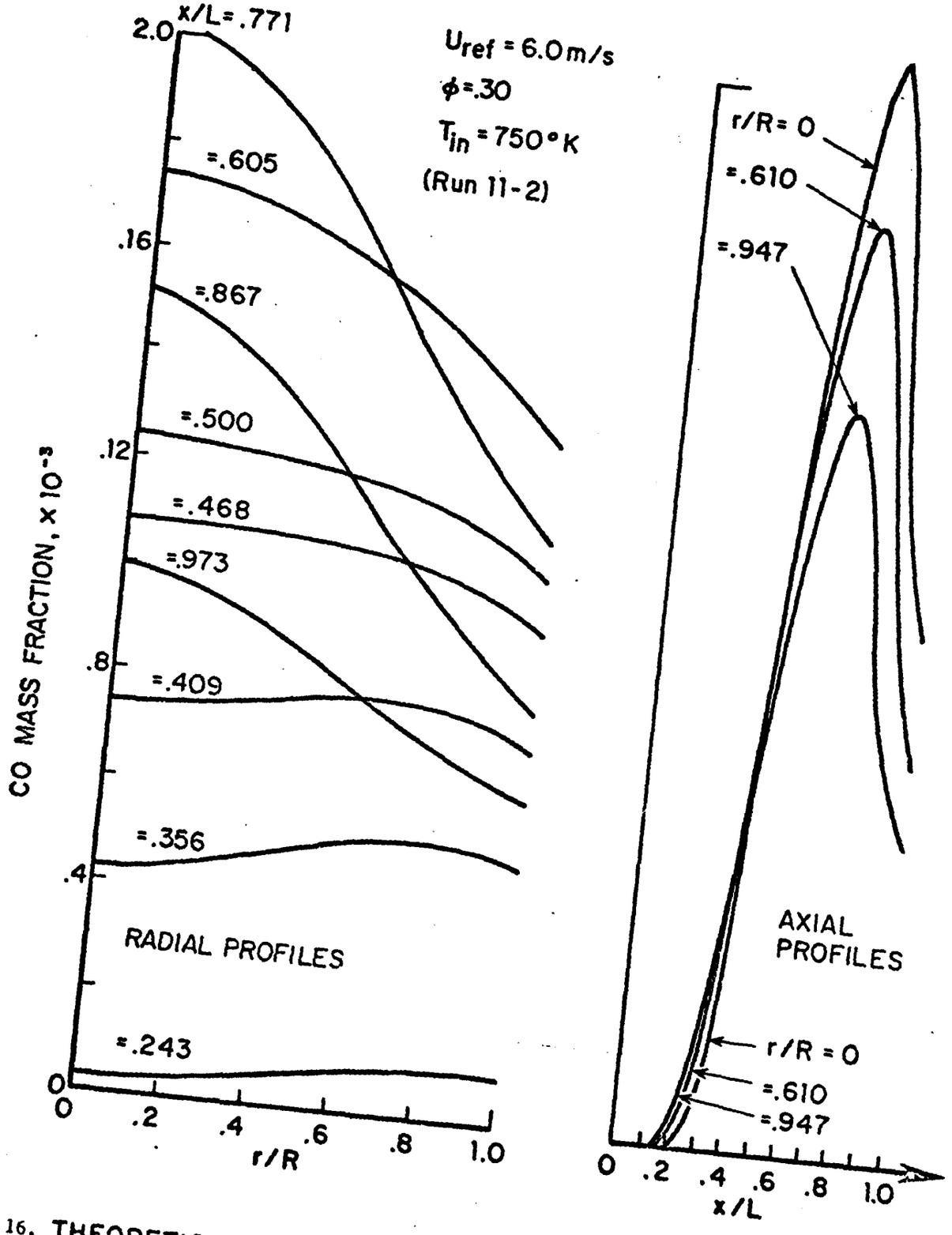

FIGURE 16. THEORETICAL PROFILES OF CO VS. r AND x FOR 3-STEP (OVERALL) CATALYTIC OXIDATION OF C_3H_8

THEORY VS. EXPERIMENTS

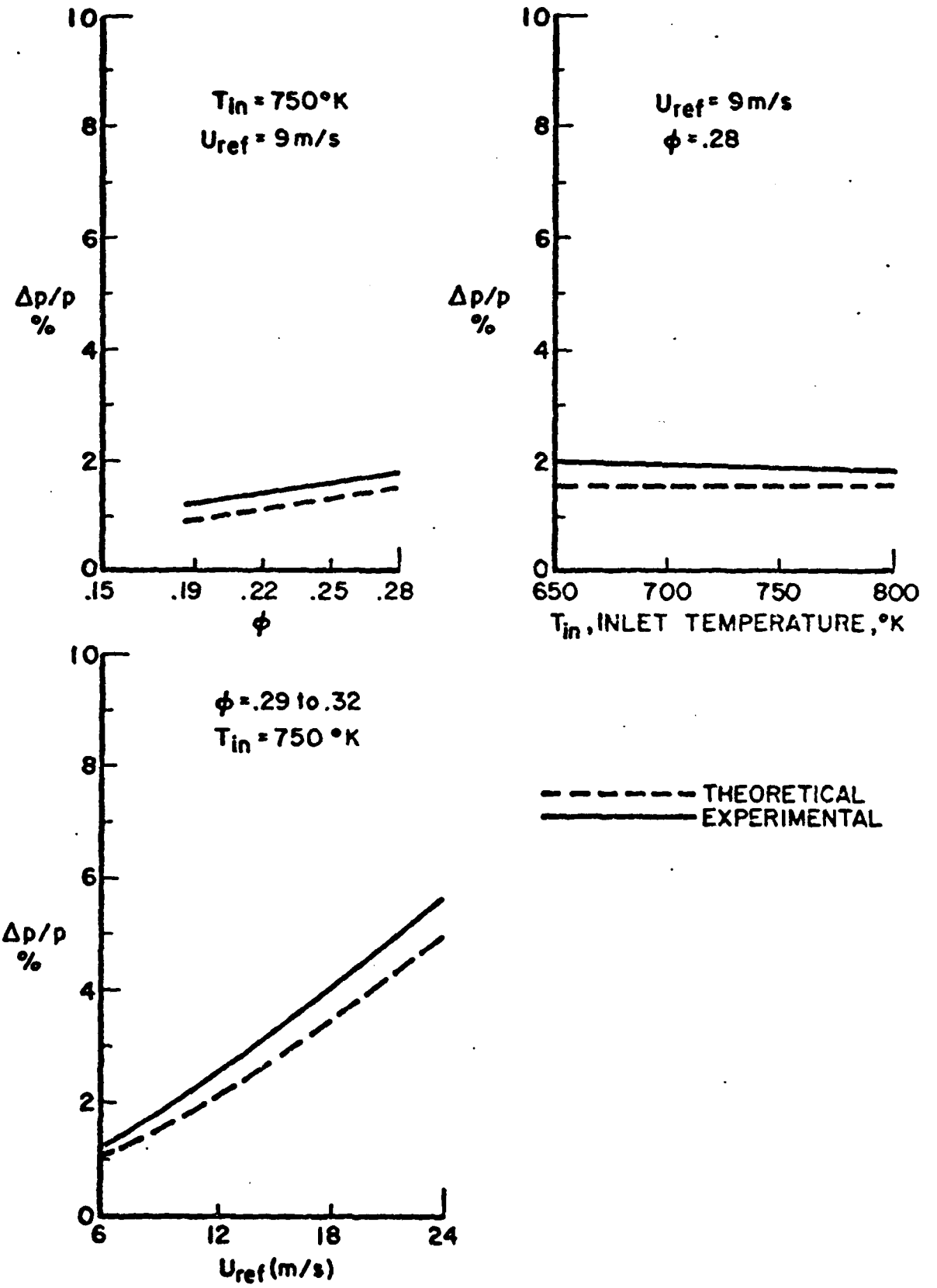

PRESSURE DROP
FIGURE 17

THEORY VS. EXPERIMENTS

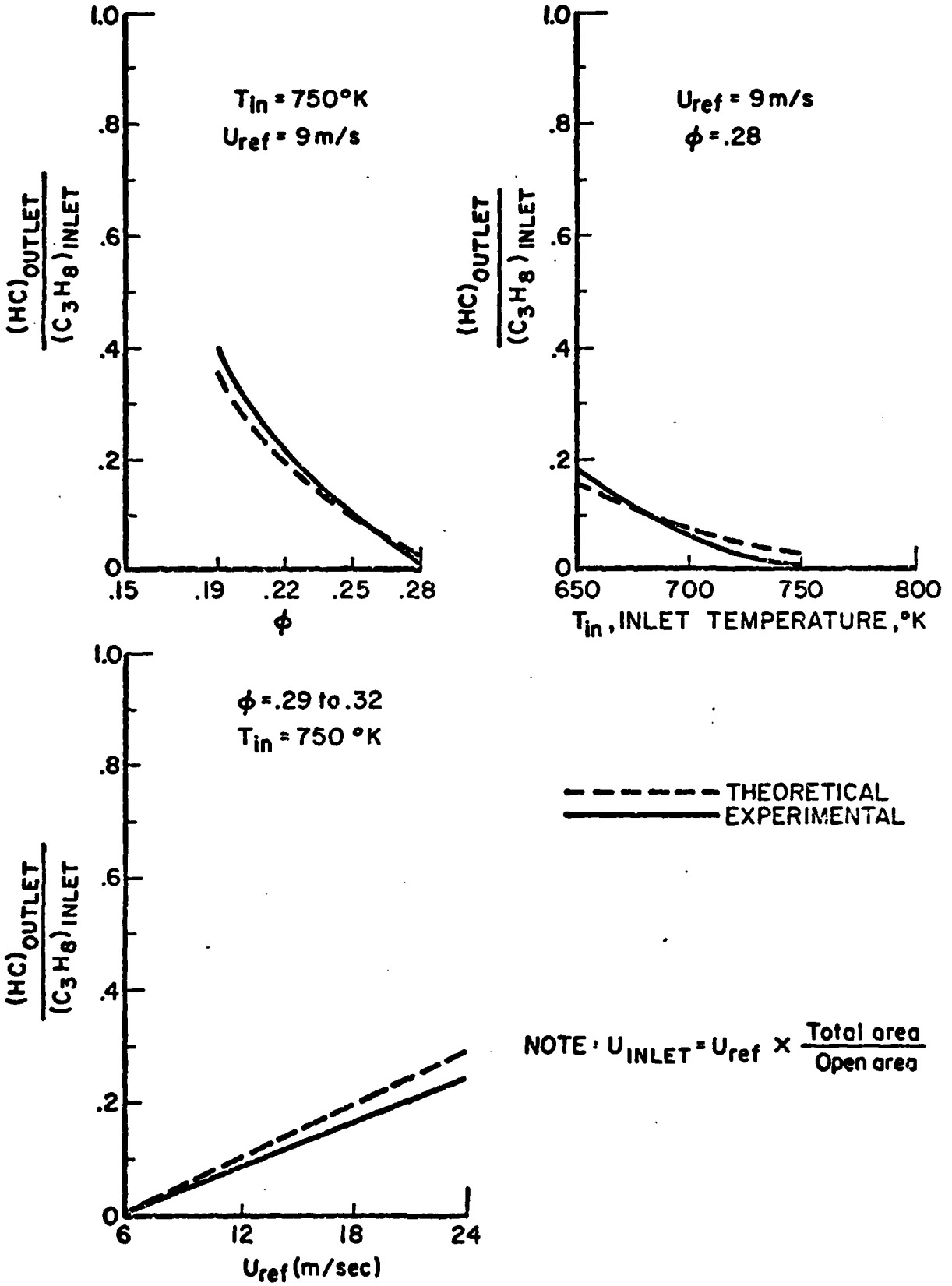

NOTE: $U_{INLET} = U_{ref} \times \frac{\text{Total area}}{\text{Open area}}$

UNBURNED HYDROCARBONS

FIGURE 18

THEORY VS. EXPERIMENTS

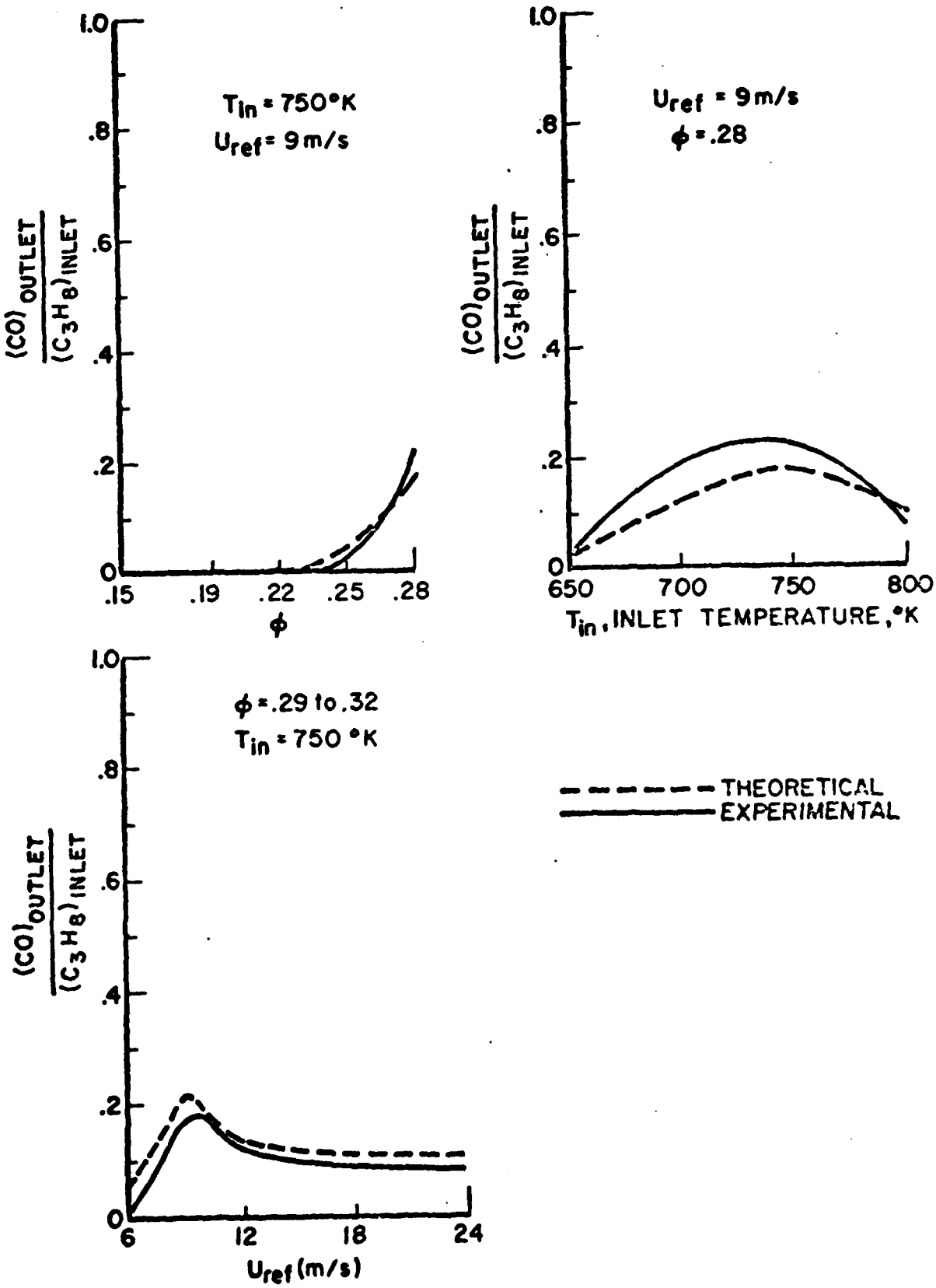

UNBURNED CO

FIGURE 19

THEORY VS. EXPERIMENTS

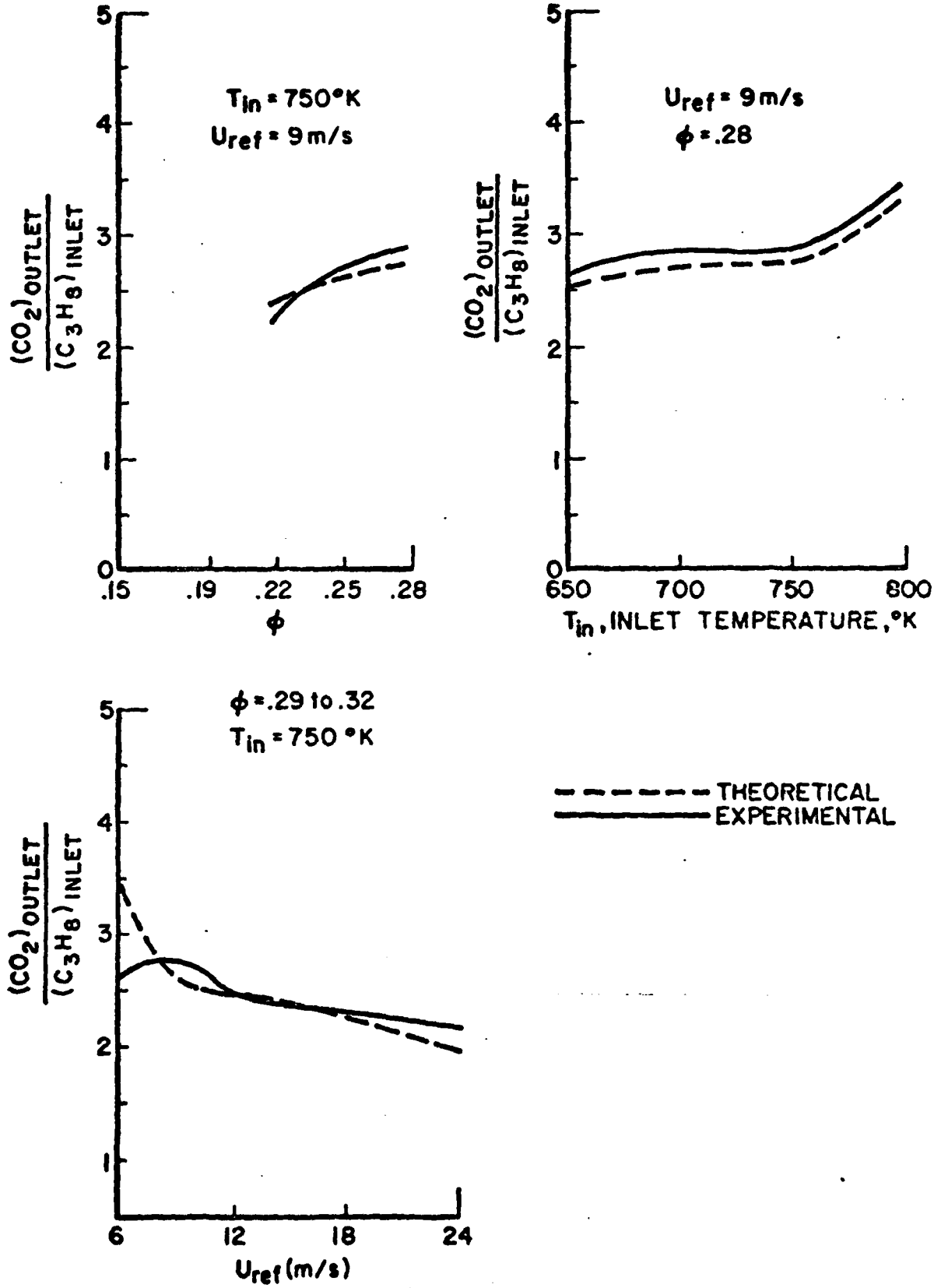

CO_2 PRODUCT

FIGURE 20

THEORY VS. EXPERIMENTS

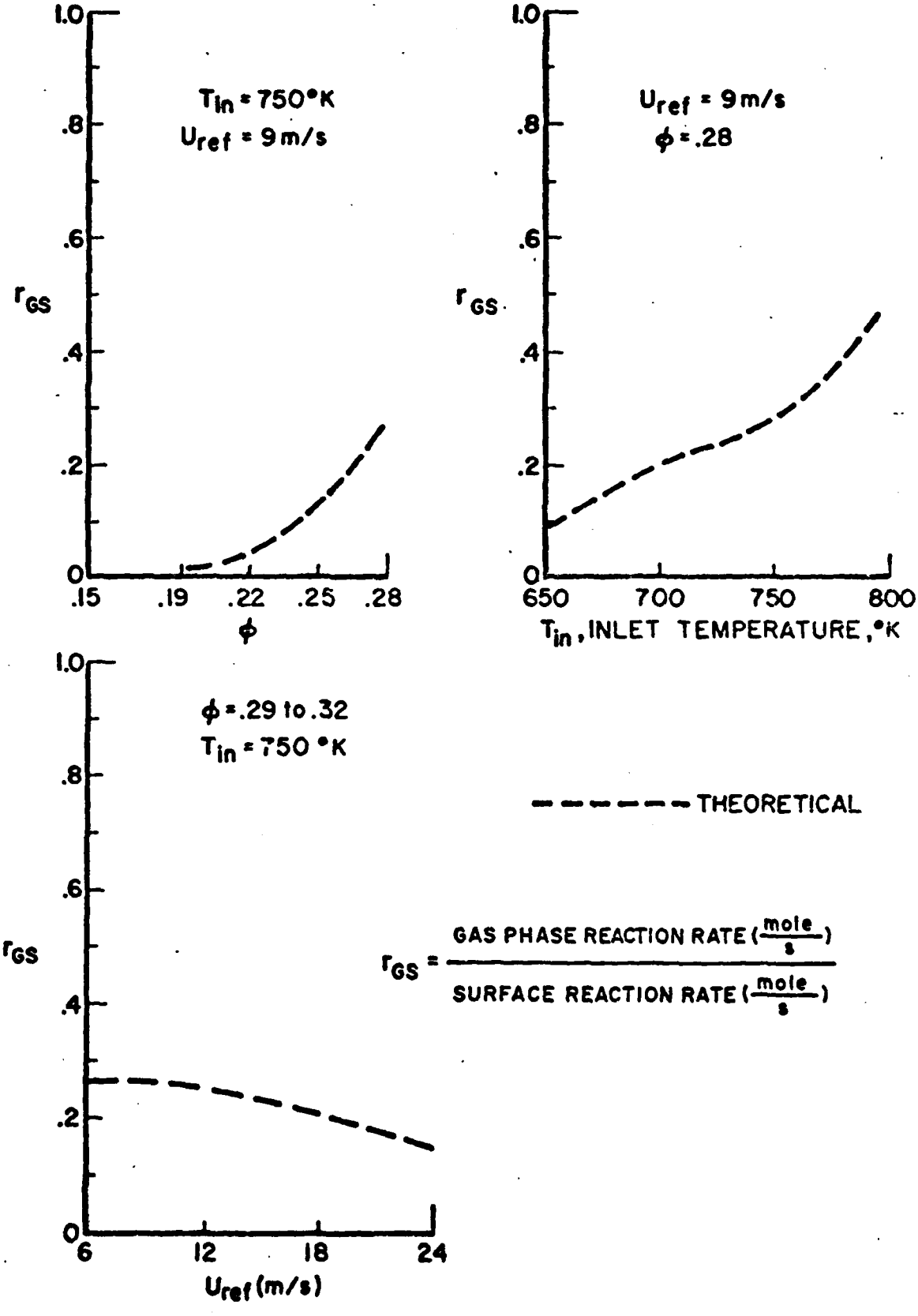

RELATIVE IMPORTANCE OF GAS PHASE VS. SURFACE REACTION RATES

FIGURE 21

FIGURE 22a. THE $\frac{t\,chem}{R^2/D_o}$ vs X/L FOR DIFFERENT Uref

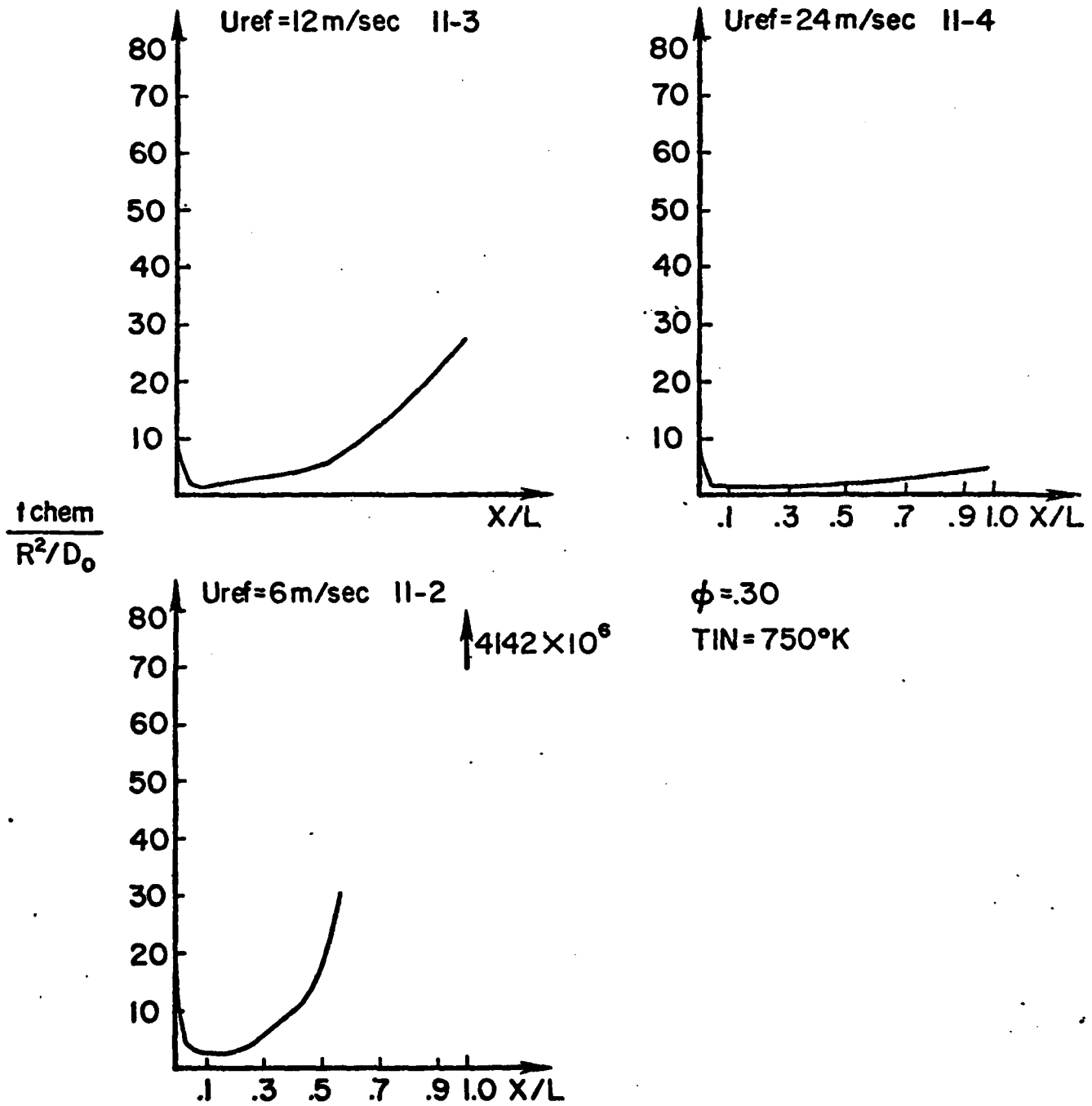

FIGURE 22b. THE $\frac{t\,chem}{R^2/D_o}$ vsX/L FOR DIFFERENT INLET TEMPERATURES

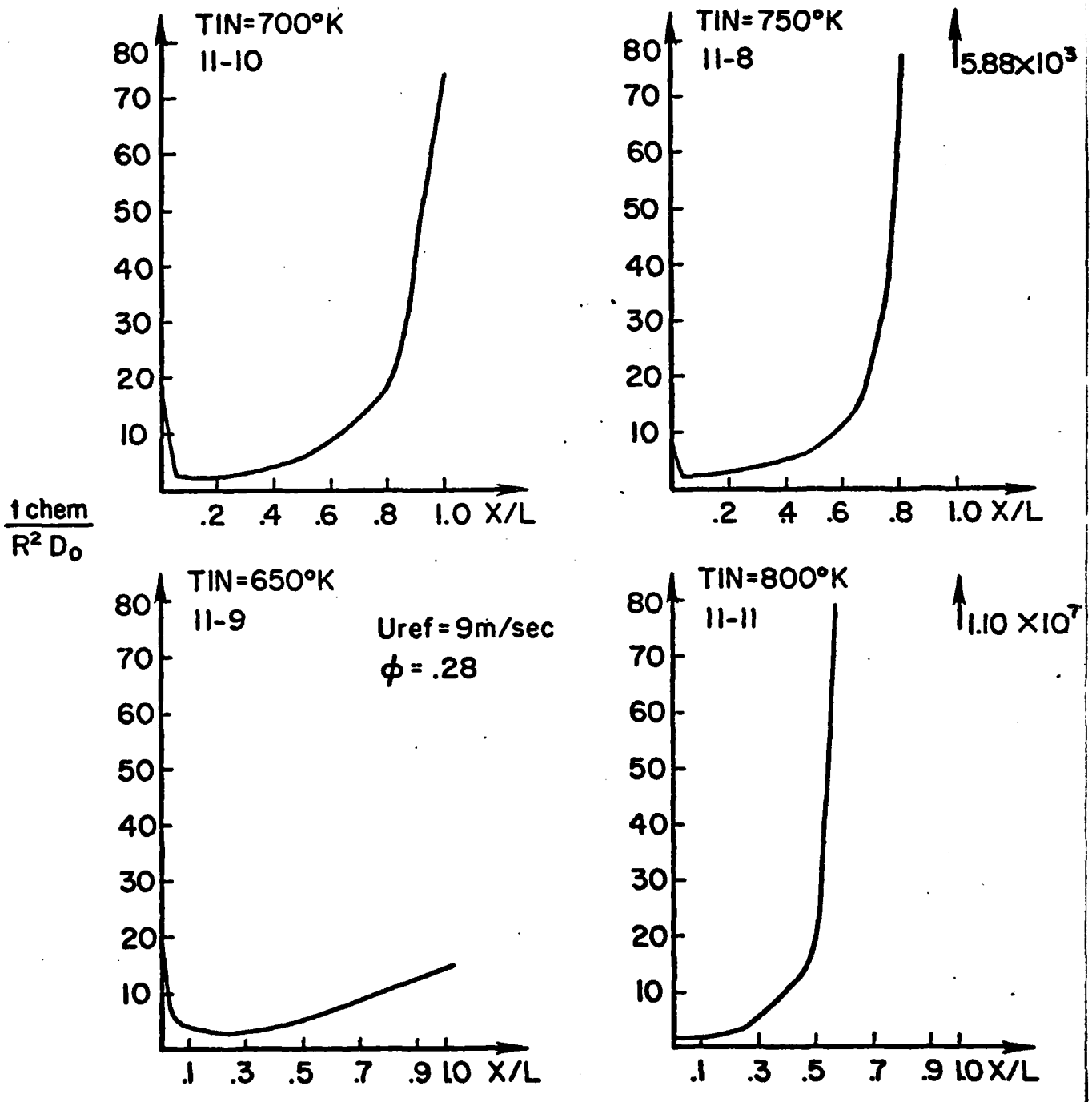

FIGURE 22c. THE $\frac{t\,chem}{R^2/D_o}$ vs X/L FOR DIFFERENT ϕ

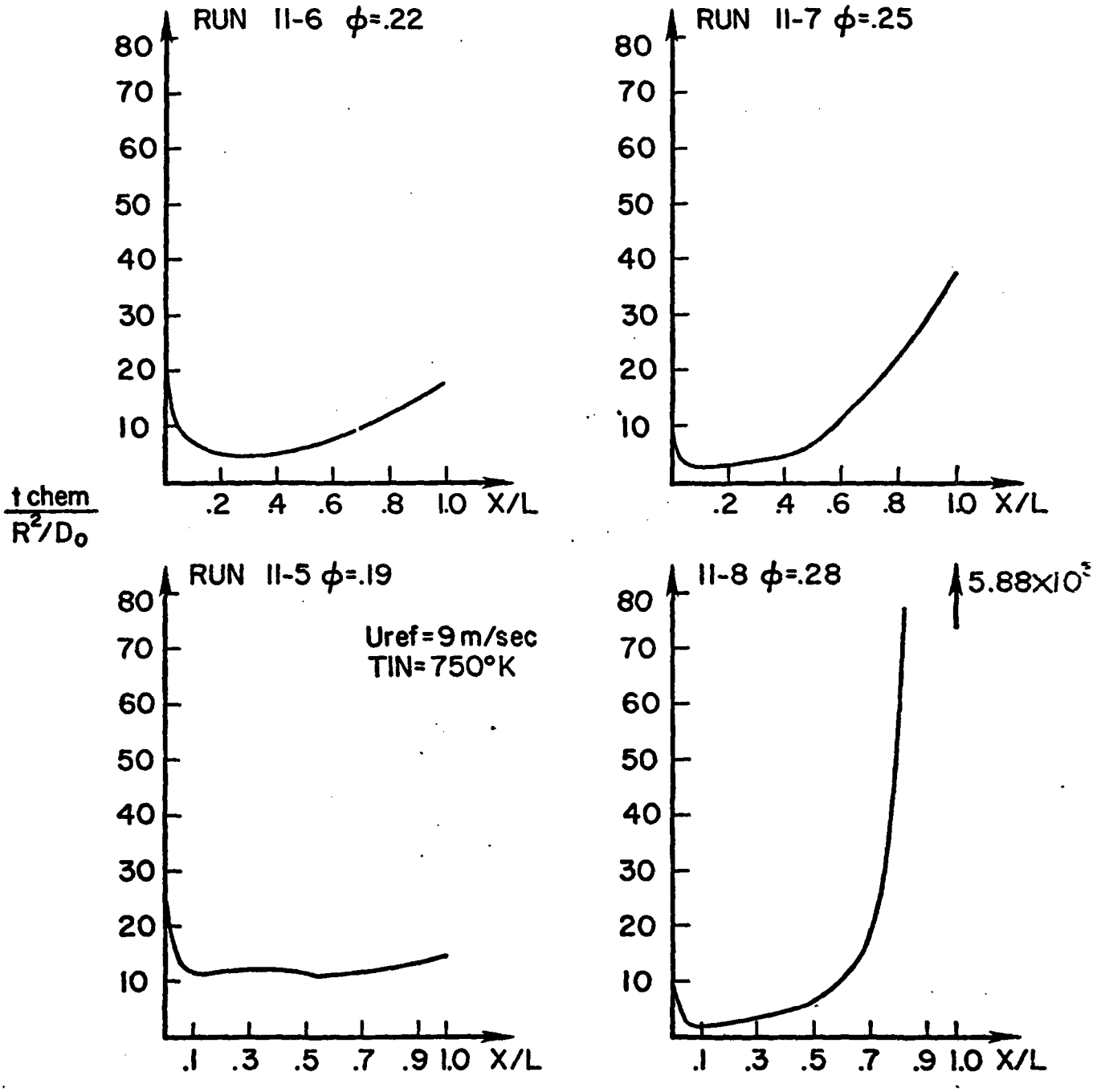

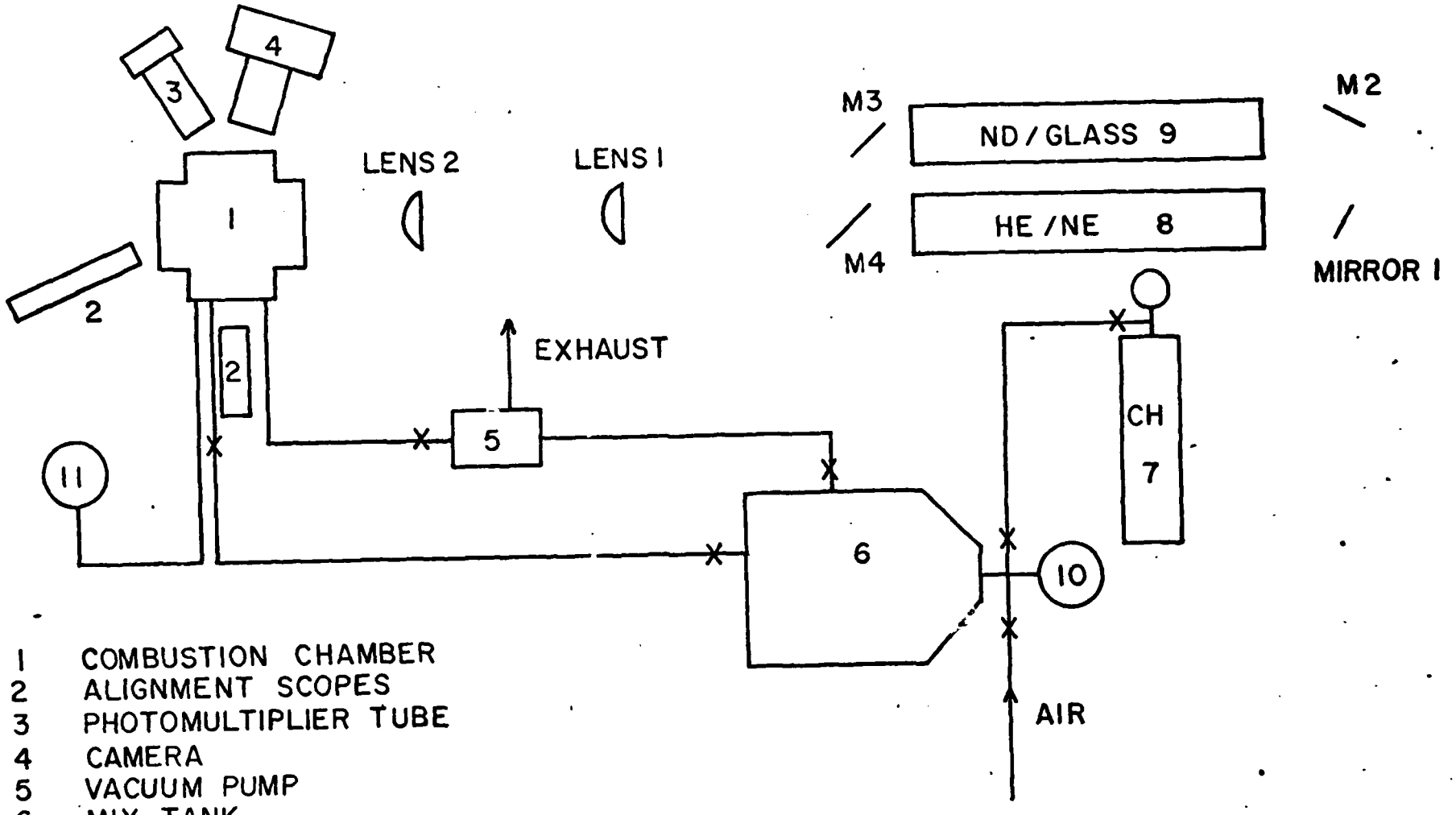

1 COMBUSTION CHAMBER
2 ALIGNMENT SCOPES
3 PHOTOMULTIPLIER TUBE
4 CAMERA
5 VACUUM PUMP
6 MIX TANK
7 METHANE CYLINDER
8 HELIUM/NEON LASER
9 ND/GLASS LASER
10 MIX TANK PRESSURE GAUGE
11 CHAMBER PRESSURE GAUGE

FIGURE 23

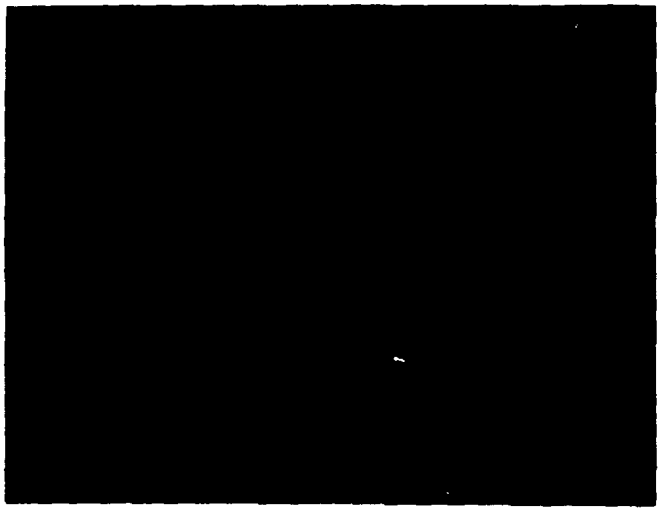

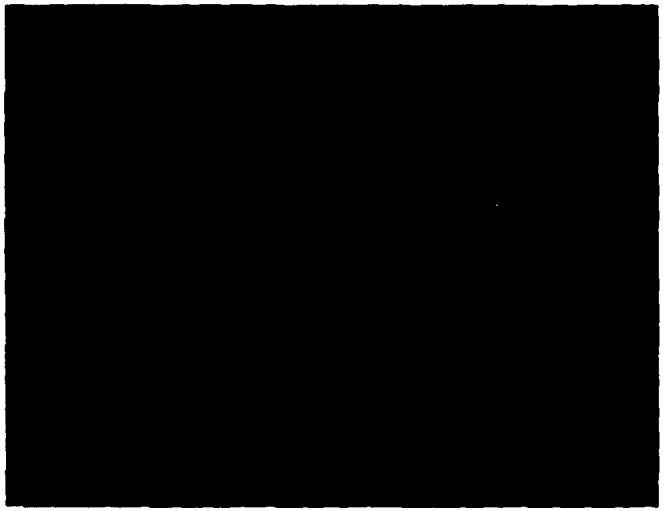

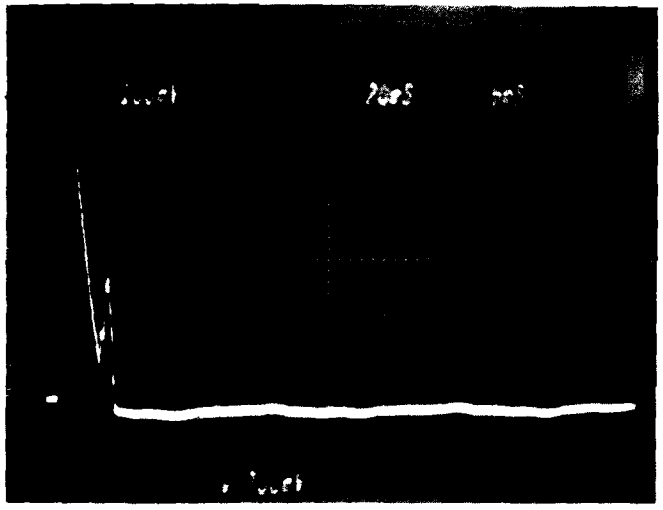

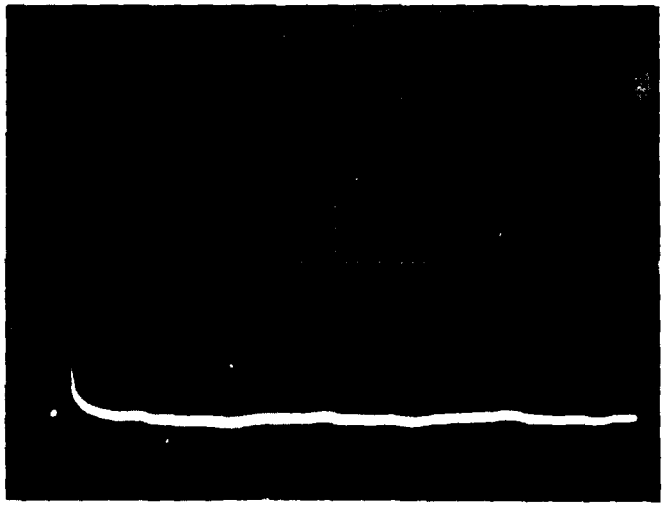

30μ PARTICLE IN AIR
LASER VOLTAGE: 880 VOLTS

30μ PARTICLE IN VACUUM
LASER VOLTAGE: 880 VOLTS

FIGURE 24

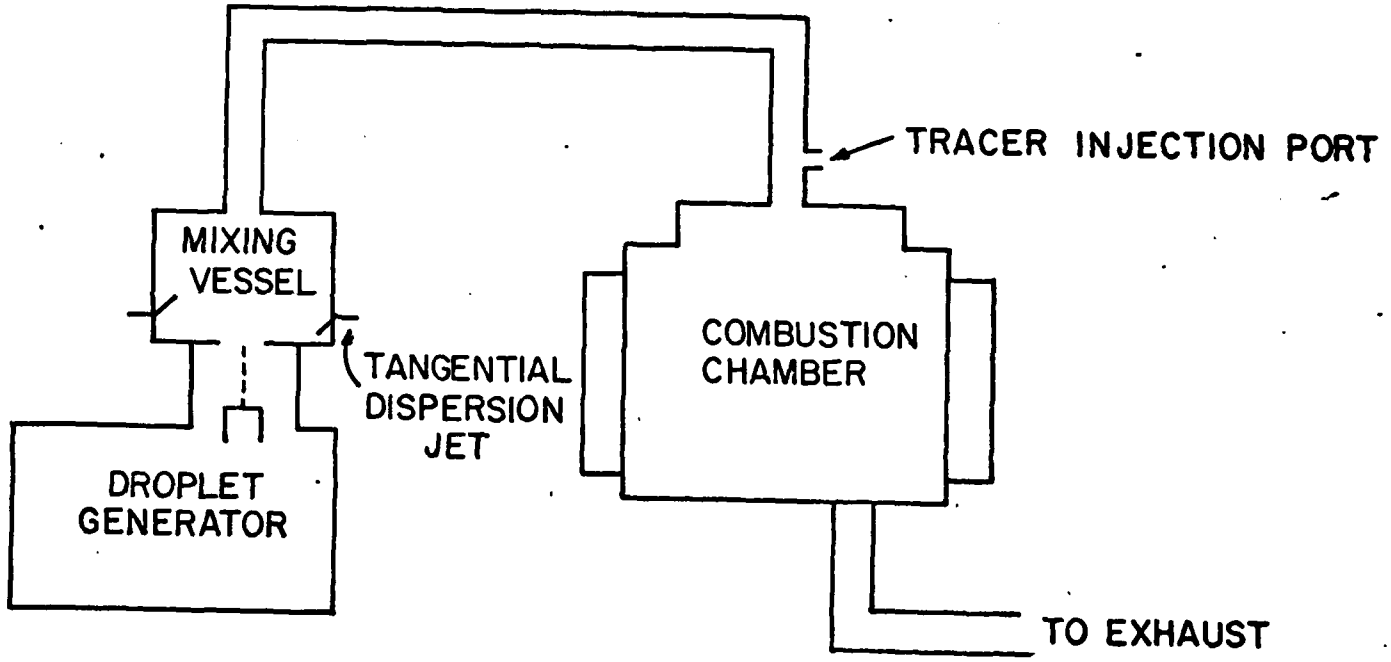
TRACER INJECTION PORT
MIXING VESSEL
TANGENTIAL DISPERSION JET
COMBUSTION CHAMBER
DROPLET GENERATOR
TO EXHAUST

FIGURE 25

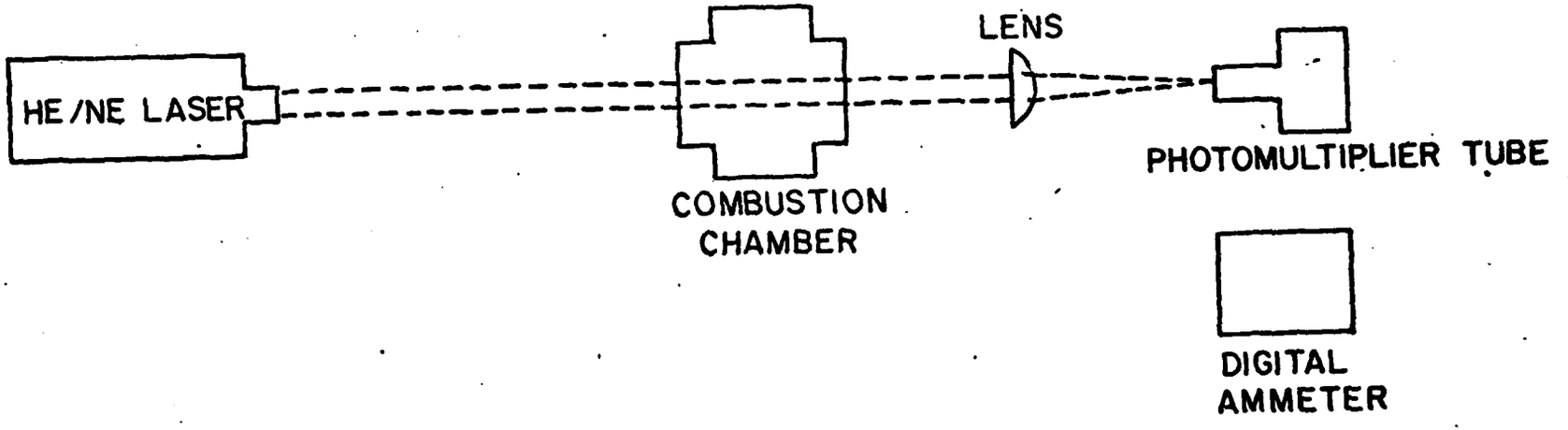
HE/NE LASER
COMBUSTION CHAMBER
LENS
PHOTOMULTIPLIER TUBE
DIGITAL AMMETER

FIGURE 26

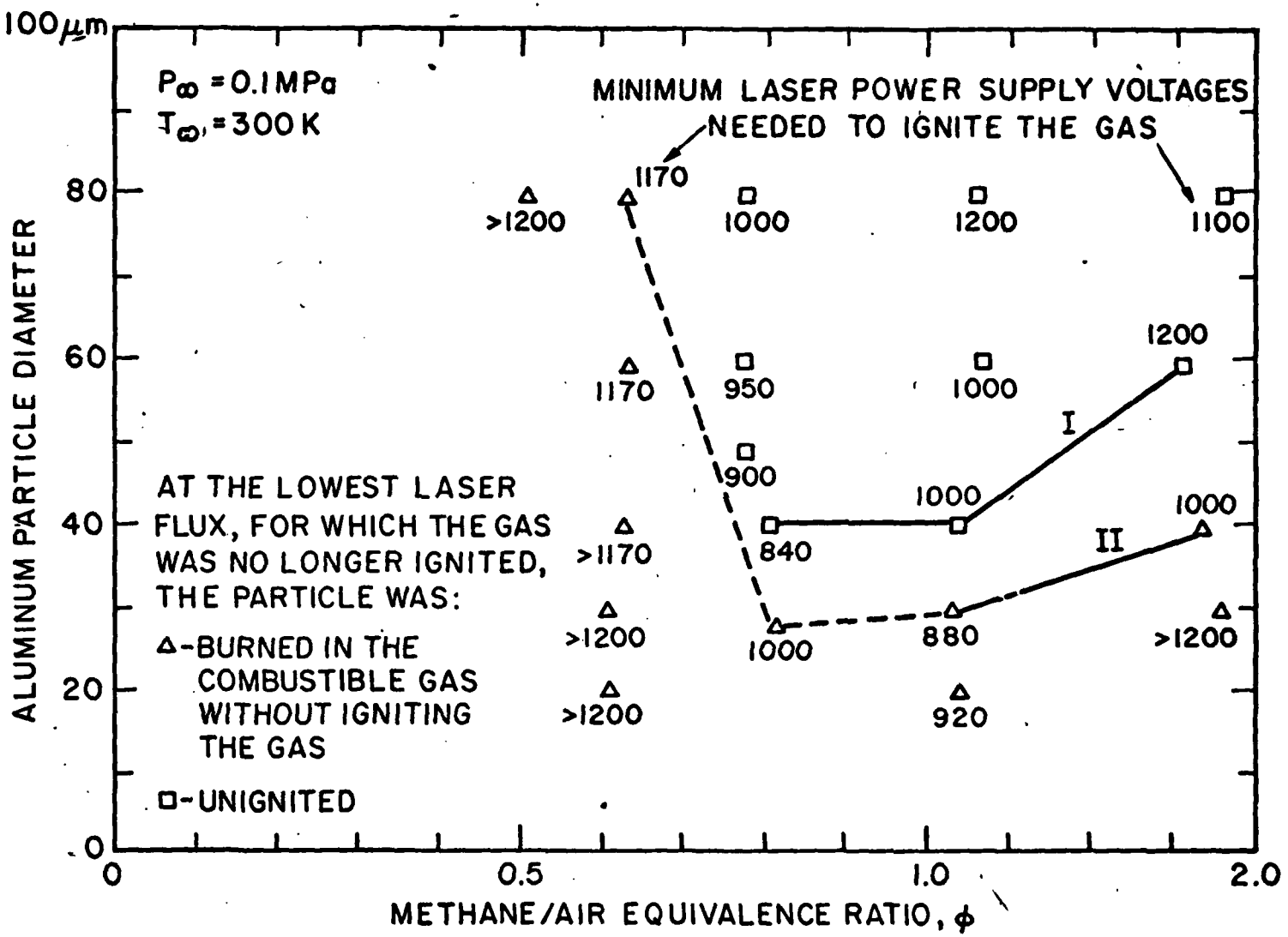
100μm
80
60
40
20
0
ALUMINUM PARTICLE DIAMETER
P_∞ = 0.1 MPa
T_∞ = 300 K
MINIMUM LASER POWER SUPPLY VOLTAGES NEEDED TO IGNITE THE GAS
AT THE LOWEST LASER FLUX, FOR WHICH THE GAS WAS NO LONGER IGNITED, THE PARTICLE WAS:
△-BURNED IN THE COMBUSTIBLE GAS WITHOUT IGNITING THE GAS
□-UNIGNITED
>1200
1170
1000
1200
1100
1170
950
1000
1200
900
I
1000
1000
>1170
840
II
>1200
1000
880
>1200
>1200
920
0
0.5
1.0
2.0
METHANE/AIR EQUIVALENCE RATIO, ϕ

FIGURE 27

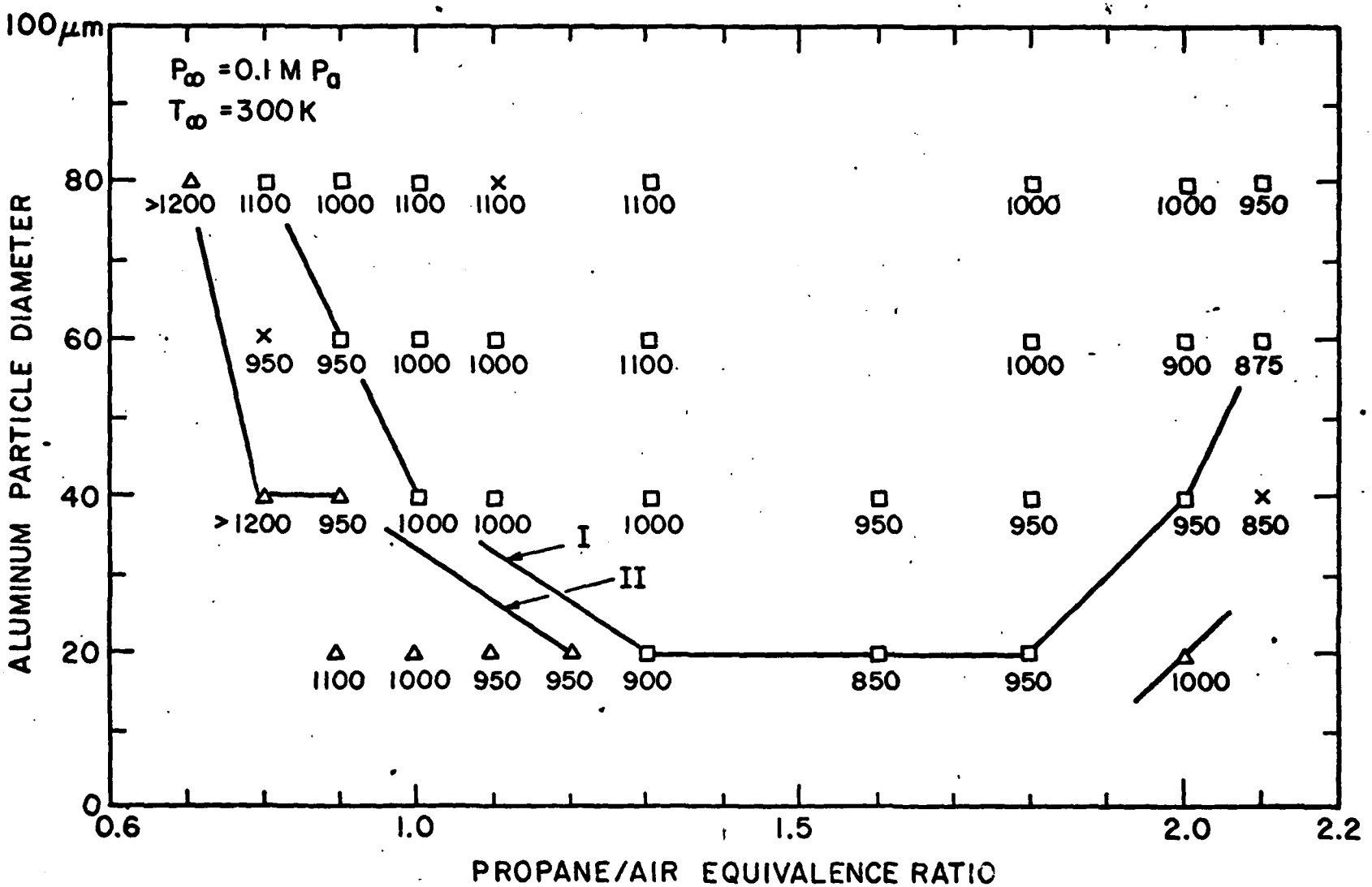
100μm
80
60
40
20
0
P_∞ = 0.1 M P_a
T_∞ = 300 K
ALUMINUM PARTICLE DIAMETER
>1200 1100 1000 1100 1100 1100 1000 1000 950
950 950 1000 1000 1100 1000 900 875
>1200 950 1000 1000 1000 950 950 950 850
1100 1000 950 950 900 850 950 1000
I
II
0.6
1.0
1.5
2.0
2.2
PROPANE/AIR EQUIVALENCE RATIO

FIGURE 28

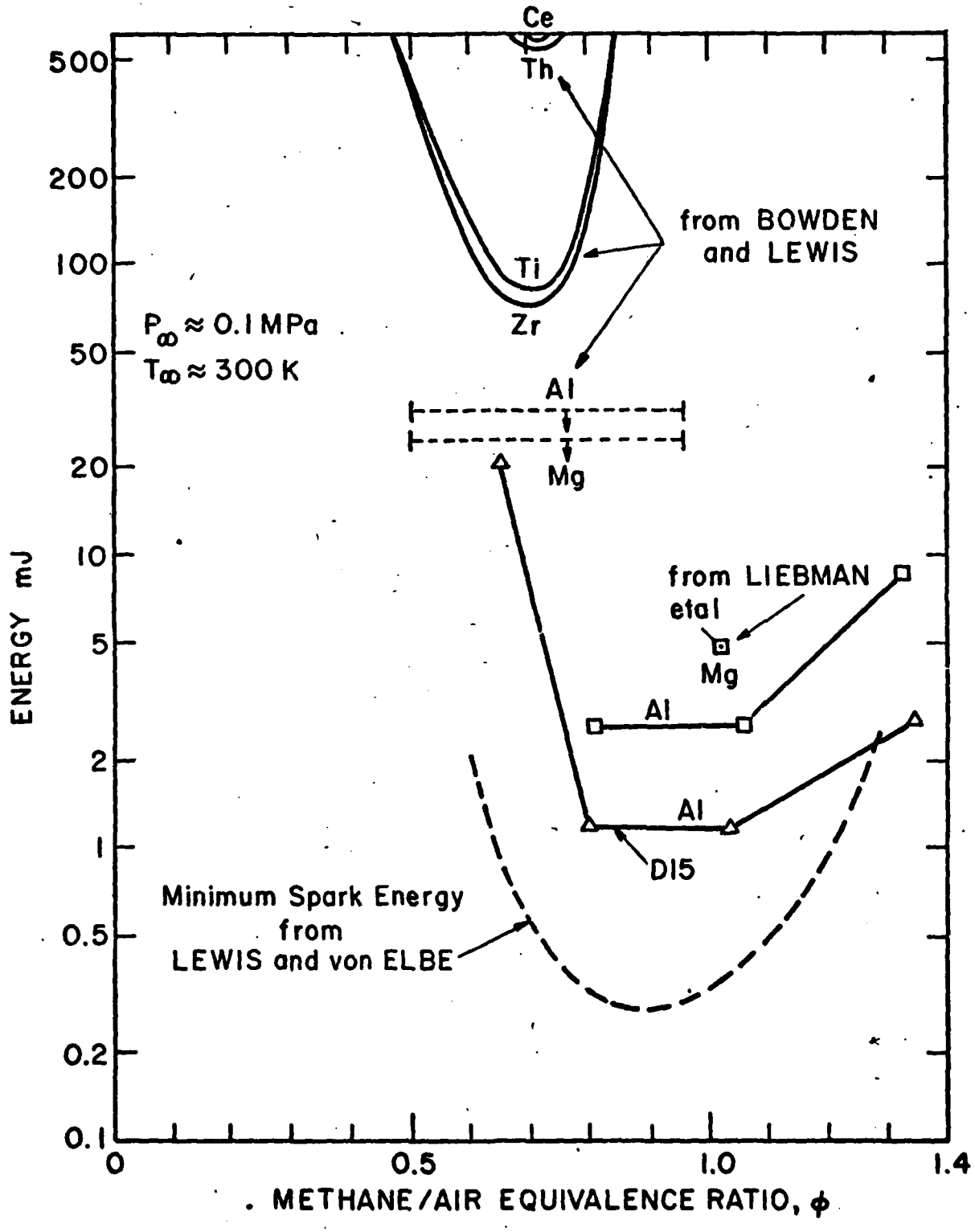
Ce
Th
Ti
Zr
from BOWDEN and LEWIS
$P_\infty \approx 0.1$ MPa
$T_\infty \approx 300$ K
Al
Mg
from LIEBMAN etal
Mg
Al
Al
D15
Minimum Spark Energy from LEWIS and von ELBE
ENERGY mJ
500
200
100
50
20
10
5
2
1
0.5
0.2
0.1
0
0.5
1.0
1.4
METHANE/AIR EQUIVALENCE RATIO, ϕ

FIGURE 29

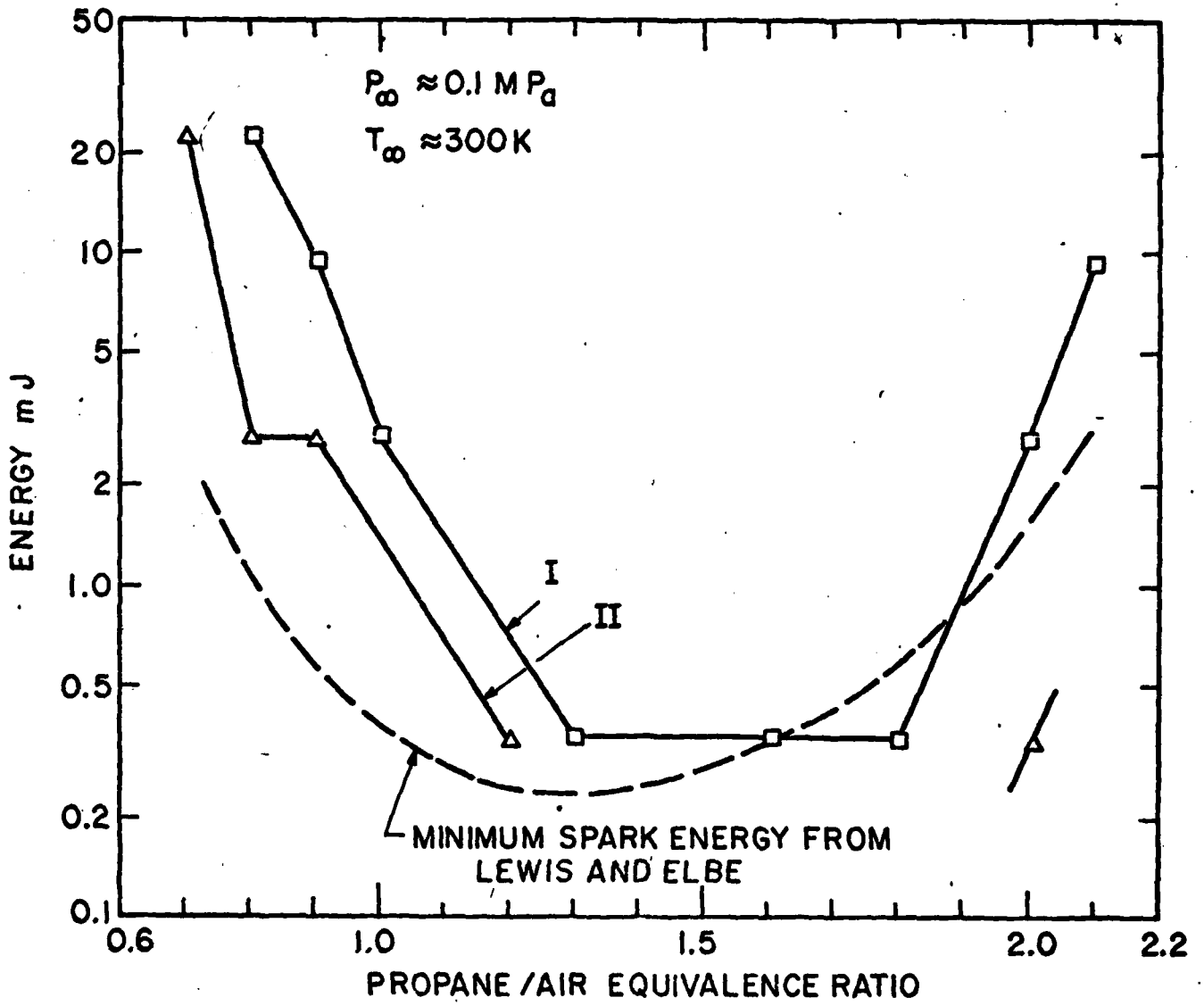
50
20
10
5
2
1.0
0.5
0.2
0.1
ENERGY mJ
$P_\infty \approx 0.1$ MPa
$T_\infty \approx 300$K
I
II
MINIMUM SPARK ENERGY FROM
LEWIS AND ELBE
0.6
1.0
1.5
2.0
2.2
PROPANE /AIR EQUIVALENCE RATIO

FIGURE 30

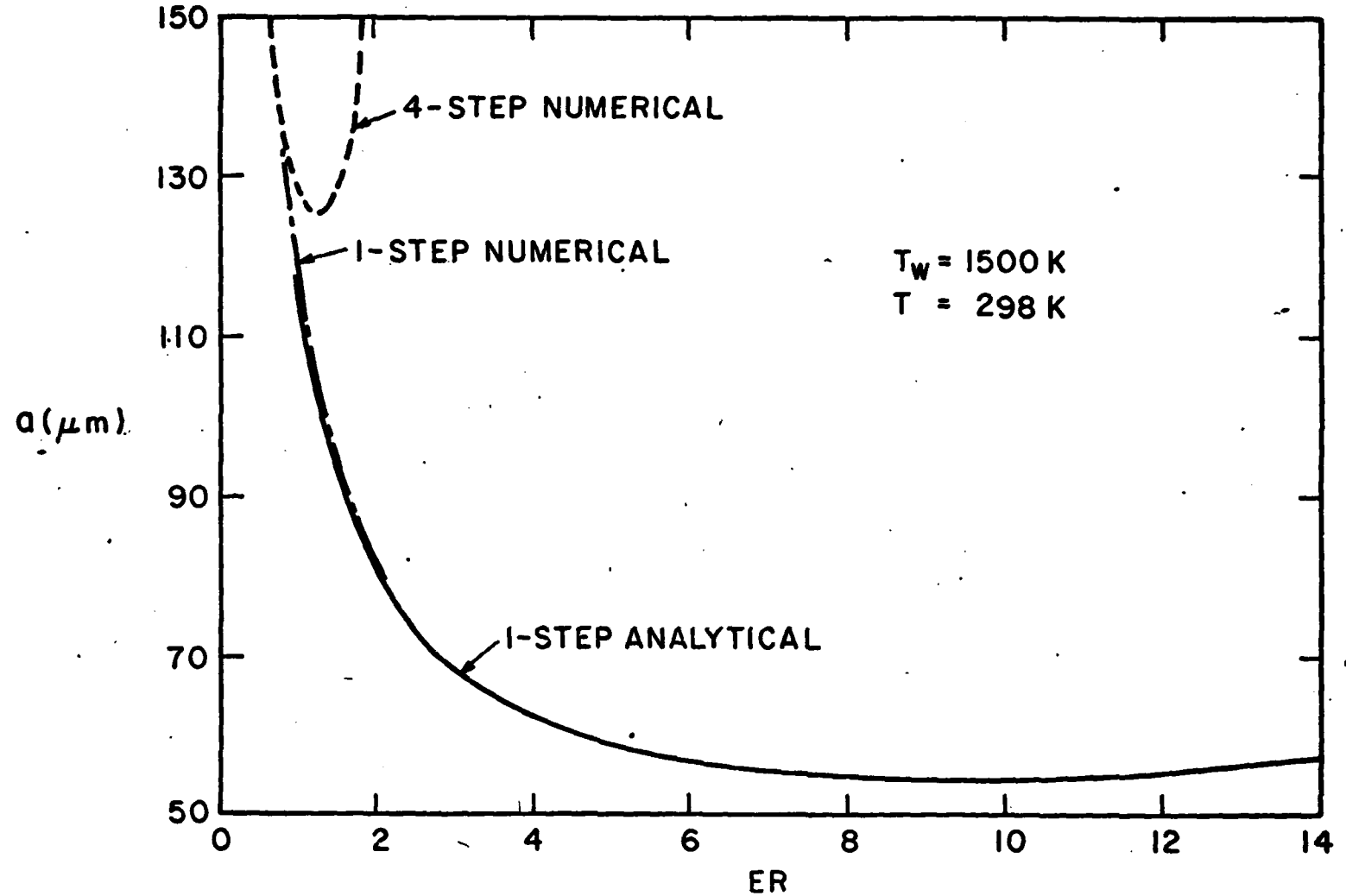

CRITICAL PARTICLE SIZE VS MIXTURE RATIO

FIGURE 31

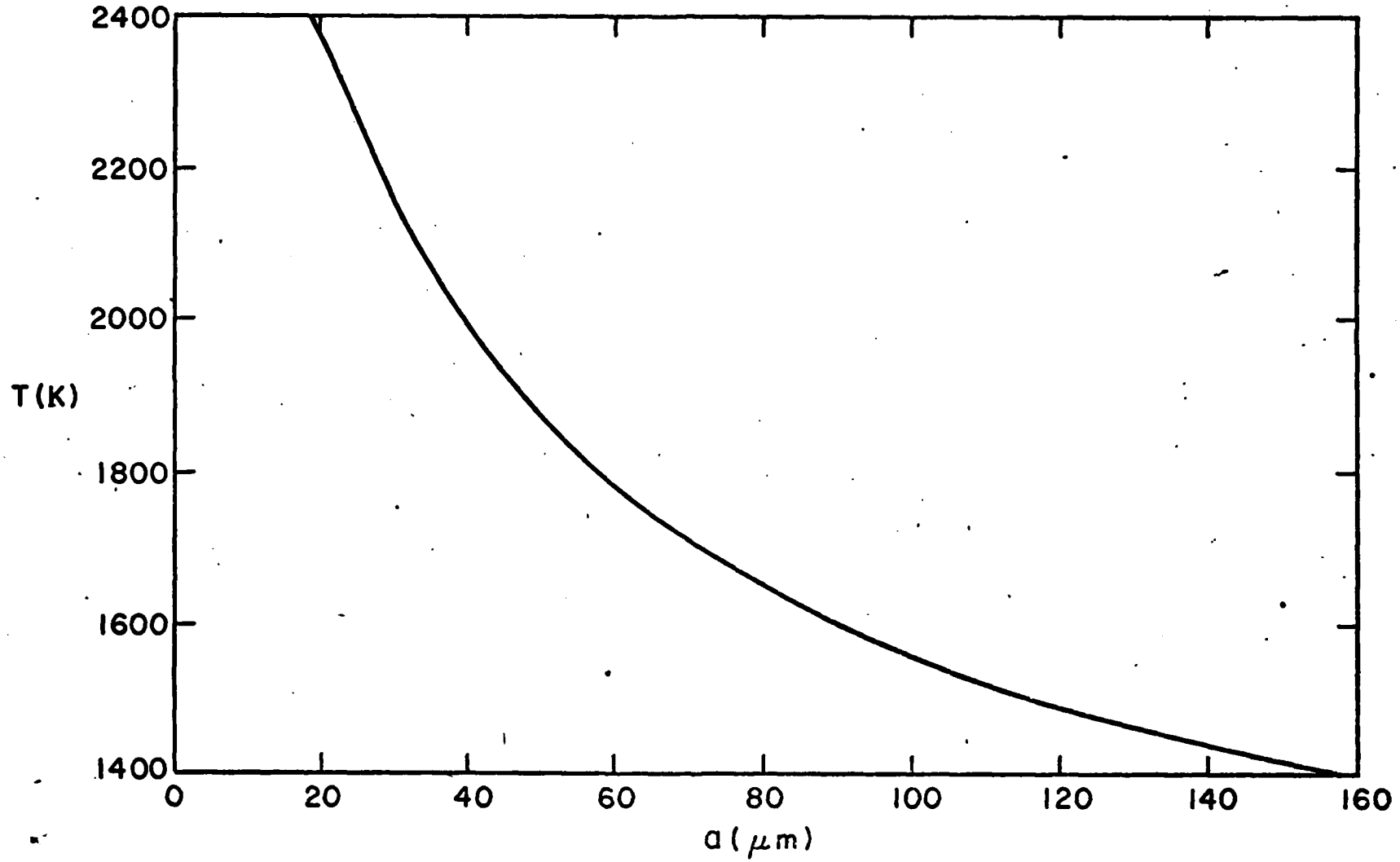

CRITICAL PARTICLE TEMPERATURE VS PARTICLE SIZE

FIGURE 32